Large-scale clustering of galaxies in general relativity

Donghui Jeong,[1] Fabian Schmidt,[1] and Christopher M. Hirata[1]

[1] *Theoretical Astrophysics, California Institute of Technology, Mail Code 350-17, Pasadena, CA 91125, USA*

(Dated: 27 July 2011)

Several recent studies have shown how to properly calculate the observed clustering of galaxies in a relativistic context, and uncovered corrections to the Newtonian calculation that become significant on scales near the horizon. Here, we retrace these calculations and show that, on scales approaching the horizon, the observed galaxy power spectrum depends strongly on which gauge is assumed to relate the intrinsic fluctuations in galaxy density to matter perturbations through a linear bias relation. Starting from simple physical assumptions, we derive a gauge-invariant expression relating galaxy density perturbations to matter density perturbations on large scales, and show that it reduces to a linear bias relation in synchronous-comoving gauge, corroborating an assumption made in several recent papers. We evaluate the resulting observed galaxy power spectrum, and show that it leads to corrections similar to an effective non-Gaussian bias corresponding to a local $f_{\rm NL,eff} \lesssim 0.5$. This number can serve as a guideline as to which surveys need to take into account relativistic effects. We also discuss the scale-dependent bias induced by primordial non-Gaussianity in the relativistic context, which again is simplest in synchronous-comoving gauge.

PACS numbers: 98.65.Dx, 98.80.Jk

I. INTRODUCTION

The clustering of galaxies and other large-scale structure (LSS) tracers on the largest scales has recently received great interest as a probe of inflation and its alternatives. In the presence of primordial non-Gaussianity, biased tracers can exhibit a significant scale-dependent bias with respect to the matter distribution which increases strongly towards large scales [1]. This can be used as a sensitive probe of primordial non-Gaussianity [2]. Furthermore, ongoing, future, and proposed surveys such as the Baryon Oscillation Spectroscopic Survey [3], the Hobby Eberly Telescope Dark Energy Experiment [4], HyperSuprime Cam, the Dark Energy Survey[1], the Subaru Prime Focus Spectrograph, BigBOSS [5], the Large Synoptic Survey Telescope[2], the Wide-Field Infrared Survey Telescope[3], Euclid[4], and the Square Kilometer Array[5] will probe modes that approach the comoving horizon using both photometric and spectroscopic galaxy surveys. All of this is strong motivation to go beyond the Newtonian picture of galaxy clustering widely adopted so far, and to embed this observable into a proper relativistic context. This is analogous to what has been done for the cosmic microwave background (CMB), and several aspects have long been worked out [6–8]. However, galaxy clustering involves a few additional complications: first, it is intrinsically three- rather than two-dimensional; second, one has to take into account selection effects such as cuts on observed flux and redshift; and third, the relation between intrinsic fluctuations in the galaxy density and the fluctuations in the matter density is non-trivial.

In order to use the clustering of LSS tracers on scales approaching the horizon $c/H(z)$, we thus need to understand the connection between the theoretical predictions for cosmological perturbations and the observationally inferred overdensities of galaxies. In particular, the perturbations in the metric, matter density, velocity, etc. are always defined with respect to a particular choice of coordinates (gauge), whereas observables should be independent of this gauge choice.

Recently, Yoo et al. [9] have shown how to calculate the observed galaxy overdensity in a generally covariant, relativistic context. In this paper, we perform a similar derivation, generalizing their results in one important aspect. On sufficiently large scales so that perturbations are linear (and assuming Gaussian initial conditions), one commonly assumes a linear relation between galaxy overdensities and perturbations in the matter density. As we show here however, the observed galaxy power spectrum depends on which gauge these overdensities are referred to. For example, [9, 10] assumed a linear bias relation in the constant-observed-redshift gauge; on the other hand, [11, 12] adopted a linear bias in synchronous-comoving gauge.

Clearly, this situation is not satisfactory, since the gauge choice should not impact *any observable* quantity. However, we can make progress using simple physical arguments. In a universe with Gaussian adiabatic perturbations, a galaxy knows about two properties of its large-scale environment: the average, "background" density of matter, and the local age (growth history) of its environment. Thus, a general bias expansion should involve *both* density and age (or local growth factor). In this context, the simplest gauge choice is the synchronous-comoving (sc) gauge, where constant-time hypersurfaces are equivalent to constant-age hypersurfaces. Then, the bias with

[1] http://www.darkenergysurvey.org/
[2] http://www.lsst.org/lsst
[3] http://wfirst.gsfc.nasa.gov/
[4] http://sci.esa.int/euclid/
[5] http://www.skatelescope.org/

respect to age becomes irrelevant, and we recover usual linear bias relation: $\delta_g^{(\rm sc)} = b\,\delta_m^{(\rm sc)}$. Further advantages of synchronous-comoving gauge are that the density field in N-body simulations is given in this gauge, and commonly used Boltzmann codes also output their results in the sc gauge. We shall thus express most of our results in synchronous-comoving gauge. The transition to other gauges can be performed easily using expressions given in the appendices. Note that when properly transformed, the results derived in different gauges should agree.

Recent papers by Challinor and Lewis [11] and Bonvin and Durrer [13] provide a further reason to reinvestigate relativistic corrections to the observed galaxy correlation, as they were not able to reach agreement with the expressions given in Ref. [9].

The outline of the paper is as follows. We begin by deriving the observed galaxy density in terms of perturbations in the synchronous-comoving gauge in Sec. II. In Sec. III, we discuss how galaxy biasing can be implemented in a gauge-invariant way. Sec. IV discusses the observed galaxy power spectrum. We conclude in Sec. V. In the appendices, we present useful results on the conversion between different gauges and metric conventions (App. A), more details on the derivations (App. B), and various analytical test cases for the expression for the observed galaxy overdensity (App. C). We also make the connection with the work of other recent papers [9–11, 13] in App. D.

II. THE OBSERVED GALAXY DENSITY IN SYNCHRONOUS GAUGE

In this section, we will compute the perturbations to the density of large scale stucture tracers to linear order.

A. Notation

Throughout, unless otherwise noted, we shall adopt the synchronous-comoving gauge. Specifically, we write

$$ds^2 = a^2(\tau)\left\{-d\tau^2 + [\,(1+2D)\,\delta_{ij} + 2E_{ij}]\,dx^i\,dx^j\right\}, \tag{1}$$

where τ is the conformal time, D is a scalar metric perturbation while E_{ij} is transverse and traceless, and related to the scalar perturbation E by

$$E_{ij} = \left(\partial_i\partial_j - \frac{1}{3}\delta_{ij}\nabla^2\right)E. \tag{2}$$

Latin letters denote the spatial indices and Greek letters denote space-time indices.

In galaxy surveys, we observe the angular position of the galaxy as well as its redshift $\tilde{z}$. Hereafter, we shall denote observed (or inferred) coordinates with a tilde. We can assign the galaxy a position $\tilde{\mathbf{x}}$ in three-dimensional cartesian coordinates via

$$\tilde{\mathbf{x}} = \tilde{\chi}\hat{\tilde{\boldsymbol{n}}}, \tag{3}$$

where $\tilde{\chi} = \bar{\chi}(\tilde{z})$ and $\bar{\chi}(z)$ is the distance-redshift relation in the background Universe[6], and $\hat{\tilde{\boldsymbol{n}}}$ is the unit vector in the direction of the observed position of the galaxy. In an unperturbed Universe, where both the observer and the galaxy are comoving with the background matter, this position in fact corresponds to the true position (in comoving coordinates). This is because the photon geodesic in an unperturbed Universe can be written as

$$\bar{x}^\mu(\chi) = (\tau_0 - \chi,\ \hat{\tilde{\boldsymbol{n}}}\chi), \tag{4}$$

where τ_0 is the conformal time at observation, and we have chosen the affine parameter to be the comoving distance (along the light ray). Thus, the space-time point of emission of the photon is given by $\bar{x}^\mu(\tilde{\chi})$.

Note that we choose the comoving distance χ as the affine parameter in Eq. (4). One convenient feature of this parametrization is that the geodesic equations with respect to χ coincide with those of conformally transformed coordinates with metric $\hat{g}_{\mu\nu} = g_{\mu\nu}/a^2$; in the case of a spatially flat FRW universe, it is simply a straight line as in Eq. (4). The corresponding affine parameter λ in the physical FRW metric $g_{\mu\nu}$ is determined through $d\lambda/d\chi \propto a^2$.

In a perturbed Universe, the true location of the galaxy is defined by the unique starting point of the geodesic which ends at the observer's location [$\tilde{\mathbf{x}}_o = (0,0,0)$], arrives out of the direction $\hat{\tilde{\boldsymbol{n}}}$, and corresponds to a photon redshift $\tilde{z}$ (see Fig. 1); in other words, the photon frequency at arrival at $\tilde{\mathbf{x}}_o$ is

$$\tilde{\nu} = \frac{\nu_0}{1+\tilde{z}}. \tag{5}$$

Here we assume we have some frequency standard ν_0 (e.g., spectral line) to compare the photon frequency to. In the next section, the perturbed photon geodesic plays the central role when connecting the observed galaxy position to the coordinate.

In the following, it is useful to define projection operators, so that for any spatial vector X^i and tensor E_{ij},

$$\begin{aligned} X_\parallel &\equiv \hat{\tilde{n}}_i X^i, \\ E_\parallel &\equiv \hat{\tilde{n}}_i\hat{\tilde{n}}_j E^{ij}, \\ X^i_\perp &\equiv (\delta^i{}_j - \hat{\tilde{n}}^i\hat{\tilde{n}}_j)X^j, \text{ and} \\ E_\perp &\equiv (\delta^{ij} - \hat{\tilde{n}}^i\hat{\tilde{n}}^j)E_{ij}. \end{aligned} \tag{6}$$

Note that for a traceless tensor E_{ij}, $E_\perp = -E_\parallel$. Correspondingly, we define projected derivative operators,

$$\begin{aligned} \partial^i_\parallel &\equiv \hat{\tilde{n}}^i\hat{\tilde{n}}^j\partial_j, \\ \partial_\parallel &\equiv \hat{\tilde{n}}^i\partial_i, \text{ and} \\ \partial^i_\perp &\equiv (\delta^{ij} - \hat{\tilde{n}}^i\hat{\tilde{n}}^j)\partial_j = \partial^i - \hat{\tilde{n}}^i\partial_\parallel. \end{aligned} \tag{7}$$

[6] Throughout, we assume that we have perfect knowledge of the background expansion history, and hence neglect Alcock-Paczyński-type distortions. These can be taken into account straightforwardly.

By taking the derivative of the unit vector $\hat{\tilde{n}}$, we find

$$\partial_j \hat{\tilde{n}}^i = \tilde{\chi}^{-1}(\delta^i_j - \hat{\tilde{n}}^i \hat{\tilde{n}}_j), \tag{8}$$

from which we derive a number of commutation relations. These include the commutators of the partial derivatives with $\hat{\tilde{n}}$:

$$[\partial_i, \hat{\tilde{n}}_j] = \partial_i \hat{\tilde{n}}_j = \tilde{\chi}^{-1}(\delta_{ij} - \hat{\tilde{n}}_i \hat{\tilde{n}}_j) \tag{9}$$

and

$$[\partial_\parallel, \hat{\tilde{n}}_i] = [\hat{\tilde{n}}^j \partial_j, \hat{\tilde{n}}_i] = \hat{\tilde{n}}^j [\partial_j, \hat{\tilde{n}}_i] + [\hat{\tilde{n}}^j, \hat{\tilde{n}}_i]\partial_j = 0. \tag{10}$$

We may also find the commutators of the derivative operators with each other. Those involving the parallel derivatives are

$$\begin{aligned} [\partial_i, \partial_\parallel] &= [\partial_i, \hat{\tilde{n}}^j \partial_j] \\ &= [\partial_i, \hat{\tilde{n}}^j]\partial_j + [\partial_i, \partial_j]\hat{\tilde{n}}^j \\ &= \tilde{\chi}^{-1}(\delta_{ij} - \hat{\tilde{n}}_i \hat{\tilde{n}}_j)\partial_j + 0 \\ &= \tilde{\chi}^{-1}\partial_{\perp i} \end{aligned} \tag{11}$$

and, since Eq. (10) shows that all components of $\hat{\tilde{n}}$ commute with $\partial_\parallel$,

$$[\partial_\parallel, \partial_{\parallel j}] = [\partial_{\parallel i}, \partial_{\parallel j}] = 0. \tag{12}$$

The perpendicular derivative satisfies

$$[\partial_{\perp i}, \partial_\parallel] = [\partial_i - \partial_{\parallel i}, \partial_\parallel] = [\partial_i, \partial_\parallel] = \tilde{\chi}^{-1}\partial_{\perp i}. \tag{13}$$

In these expressions, $\tilde{\chi}$ is the norm of the position vector so that $\hat{\tilde{n}}^i = x^i/\tilde{\chi}$. These relations are the analogue of the Christoffel symbols of spherical polar coordinates.

We also define the projection of the Laplacian operator ($\nabla^2 = \partial_i \partial^i$) as

$$\begin{aligned} \partial^2_\parallel &\equiv \partial_{\parallel i}\partial^i_\parallel = \partial_\parallel \partial_\parallel \text{ and} \\ \nabla^2_\perp &\equiv \partial_{\perp i}\partial^i_\perp = \nabla^2 - \partial^2_\parallel - \frac{2}{\tilde{\chi}}\partial_\parallel. \end{aligned} \tag{14}$$

Finally, we make use of

$$\partial_i X^i = \partial_\parallel X_\parallel + \partial_{\perp\, i} X^i_\perp + X_\parallel \partial_i \hat{\tilde{n}}^i \tag{15}$$

and

$$\partial_\parallel \hat{\tilde{n}}^i = \hat{\tilde{n}}^i \partial_{\perp i} = 0. \tag{16}$$

B. Photon geodesics

We can write the perturbed photon geodesic as

$$x^\mu(\chi) = \bar{x}^\mu(\chi) + \delta x^\mu(\chi); \tag{17}$$

here δx^μ is the perturbation to the photon path (note that the value of the affine parameter at emission is no longer given by $\tilde{\chi}$; see Fig. 1). For our choice of affine parameter χ, we have in the unperturbed Universe [Eq. (4)]

$$\frac{d\bar{x}^\mu}{d\chi} = (-1, \hat{\tilde{\boldsymbol{n}}}), \tag{18}$$

while for the perturbed case [Eq. (17)] we define

$$\frac{dx^\mu}{d\chi} = (-1 + \delta\nu,\ \hat{\tilde{\boldsymbol{n}}} + \delta\boldsymbol{e}). \tag{19}$$

In terms of our affine parameter χ, the first-order geodesic equations for the fractional frequency perturbation $\delta\nu \equiv d\delta x^0/d\chi$, and the fractional perturbations to the photon momentum $\delta e^i \equiv d\delta x^i/d\chi$ are then given by

$$\frac{d}{d\chi}\delta\nu = -(D' + E'_\parallel) \tag{20}$$

and

$$\begin{aligned} \frac{d}{d\chi}\delta e^i + 2\frac{d}{d\chi}\left(D\hat{\tilde{n}}^i + E^i{}_j\hat{\tilde{n}}^j\right) &= D^{,i} + E_{jk}{}^{,i}\hat{\tilde{n}}^j\hat{\tilde{n}}^k \\ &= D^{,i} + (E_\parallel)^{,i} - \frac{2}{\chi}\left(E^i{}_k\hat{\tilde{n}}^k - E_\parallel\hat{\tilde{n}}^i\right). \end{aligned} \tag{21}$$

Note that the projection onto $\hat{\tilde{n}}$ and the spatial derivative do not commute. In the following, we denote $E^{,i}_\parallel \equiv$

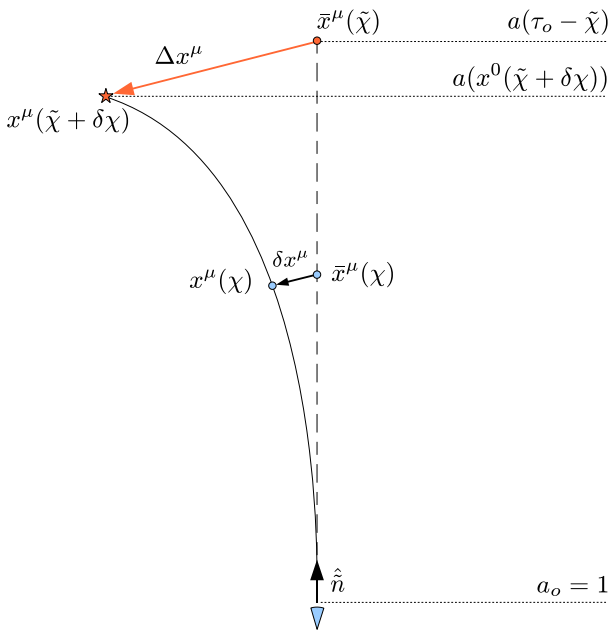

FIG. 1: Sketch of perturbed photon geodesics illustrating our notation. The observer is located at the bottom. The solid line indicates the actual photon geodesic tracing back to the source indicated by a star. The dashed line shows the apparent background photon geodesic tracing back to an inferred source position indicated by a circle.

$(E_\parallel)^{\cdot,i}$, i.e. in case of apparently ambiguous notation, the projection is taken before the derivative. Here, primes denote derivatives with respect to τ, and $d/d\chi = \partial_\parallel - \partial_\tau$. These equations are to be compared with Eqs. (9) and (12) in [9], respectively; note that $\chi_{\rm there} = -\chi_{\rm here}$ and $\delta\nu_{\rm there} = -\delta\nu_{\rm here}$.

Before integrating Eqs. (20,21), we need to determine the correct boundary conditions at the observer's position $\chi = 0$. The observer's frame of reference is described by an orthonormal tetrad e^a_μ. In terms of this basis, the components of the unit vector $\hat{\tilde{\boldsymbol{n}}}$ of the observed photon are given by

$$\hat{\tilde{n}}^a = \frac{e^a_\mu p^\mu}{p}, \tag{22}$$

where p^μ is the observed photon momentum and $p = p_i p^i$. Using the metric Eq. (1) together with the orthonormality condition

$$g^{\mu\nu} e^a_\mu e^b_\nu = \eta^{ab}, \tag{23}$$

we obtain

$$\begin{aligned} e^0_\mu &= (-1,0,0,0) \text{ and} \\ e^i_\mu &= \left(0,\, (1+D_o)\delta^i{}_j + E^i_{o\,j}\right), \end{aligned} \tag{24}$$

where a subscript o indicates a quantity evaluated at the observer's position. Inserting this into Eq. (22), and requiring that $\hat{\tilde{n}}^a$ match the observed direction of the photon, we obtain the following perturbations to the photon momentum at the observer's position ($\chi = 0$):

$$\delta\nu_o = 0 \;\text{ and }\; \delta e^i_o = -D_o \hat{\tilde{n}}^i - E^i_{o\,j}\hat{\tilde{n}}^j. \tag{25}$$

We now integrate the spatial component Eq. (21), enforcing Eq. (25) as boundary condition at $\chi = 0$:

$$\begin{aligned} \delta e^i(\chi) = &-2(D\hat{\tilde{n}}^i + E^i{}_j\hat{\tilde{n}}^j)_\chi \\ &+ \int_0^\chi d\chi' \left[D^{\cdot,i} + E^{\cdot,i}_\parallel - \frac{2}{\chi'}\left(E^i{}_k\hat{\tilde{n}}^k - E_\parallel\hat{\tilde{n}}^i\right)\right] \\ &+ (D\hat{\tilde{n}}^i + E^i{}_j\hat{\tilde{n}}^j)_o. \end{aligned} \tag{26}$$

Integrating again up to $\tilde\chi$ yields the displacements δx^i:

$$\begin{aligned} \delta x^i(\tilde\chi) &= \int_0^{\tilde\chi} d\chi\; \delta e^i \\ &= \tilde\chi(D\hat{\tilde{n}}^i + E^i{}_j\hat{\tilde{n}}^j)_o \\ &\quad + \int_0^{\tilde\chi} d\chi \left\{-2(D\hat{\tilde{n}}^i + E^i{}_j\hat{\tilde{n}}^j)\right. \\ &\quad \left. + (\tilde\chi - \chi)\Big[D^{\cdot,i} + E^{\cdot,i}_\parallel - \frac{2}{\chi}(E^i{}_k\hat{\tilde{n}}^k - E_\parallel\hat{\tilde{n}}^i)\Big]\right\}. \end{aligned} \tag{27}$$

Integrating the time-component Eq. (20) of the geodesic equation yields

$$\delta\nu(\tilde\chi) = -\int_0^{\tilde\chi} d\chi\; (D' + E'_\parallel). \tag{28}$$

This frequency shift contains the Doppler, Sachs-Wolfe, and integrated Sachs-Wolfe effects [6], as shown in App. B 1. Noting that $dx^0/d\chi = -1 + \delta\nu$, we then obtain the time delay

$$\delta x^0(\tilde\chi) = \int_0^{\tilde\chi} d\chi\; \delta\nu = -\int_0^{\tilde\chi} d\chi\; (\tilde\chi - \chi)(D' + E'_\parallel). \tag{29}$$

In order to obtain the perturbations to the source position, we need to relate the affine parameter at emission to the observed redshift. Recall that in synchronous-comoving gauge, the comoving observers' four-velocity is given by $u_\mu = (a,0,0,0)$. Then, the redshift along the perturbed geodesic at affine parameter χ is given by

$$\begin{aligned} 1 + z(\chi) &= \frac{(a^{-2}\, u_\mu\, dx^\mu/d\chi)_\chi}{(a^{-2}\, u_\mu\, dx^\mu/d\chi)_o} \\ &= \frac{[-1 + \delta\nu(\chi)]/a(x^0(\chi))}{-1} = \frac{1+\delta z}{a(x^0(\chi))}. \end{aligned} \tag{30}$$

In the second line, we have set $a_o = 1$ and defined

$$\delta z(\tilde\chi) \equiv -\delta\nu(\tilde\chi) = \int_0^{\tilde\chi} d\chi\; (D' + E'_\parallel). \tag{31}$$

For a given source observed at redshift $\tilde z$, Eq. (30) is an implicit relation for the affine parameter χ_e at emission,

$$1 + z(\chi_e) = 1 + \tilde z, \tag{32}$$

which defines the space-time location of the source through $x^\mu_{\rm source} = x^\mu(\chi_e)$. Note that since the conformal time of emission is $\tau = x^0(\chi_e)$, the redshift $\bar z(\chi_e)$ that would have been observed for the same source without any perturbations along the line of sight is given by $1/[1 + \bar z(\chi_e)] = a(x^0(\chi))$. Hence, Eq. (30) at $\chi = \chi_e$ can also be written as

$$1 + \tilde z = (1 + \bar z)(1 + \delta z(\chi_e)). \tag{33}$$

To zeroth order (in the background), $z(\chi) = \bar z(\chi)$, and hence $\chi_e = \tilde\chi$. We can then expand $\chi_e = \tilde\chi + \delta\chi$, and Eq. (30) at first order yields

$$1 + \tilde z = (1 + \tilde z)[1 - (aH)_{\tilde z}(\delta x^0 - \delta\chi) + \delta z]. \tag{34}$$

Solving this for the perturbation to the affine parameter, we obtain

$$\delta\chi = \delta x^0 - \frac{1+\tilde z}{H(\tilde z)}\delta z. \tag{35}$$

Finally, given Eq. (17), we can relate the observed position $\tilde{\mathbf{x}}$, inferred assuming unperturbed geodesics $\bar x^\mu$, and the true position $\mathbf{x}$ through (see Fig. 1)

$$\mathbf{x} = \tilde{\mathbf{x}} + \Delta\mathbf{x} = \tilde{\mathbf{x}} + \tilde\chi\delta\hat{\tilde{\boldsymbol{n}}} + \frac{d\bar{\mathbf{x}}}{d\chi}\delta\chi. \tag{36}$$

Separating into longitudinal and perpendicular parts, we obtain

$$\Delta x_\parallel = \delta x^i(\tilde\chi)\hat{\tilde n}_i + \delta\chi = \delta x_\parallel + \delta x^0 - \frac{1+\tilde z}{H}\delta z \tag{37}$$

and

$$\Delta x^i_\perp = \delta x^i - \hat{\tilde{n}}^i \delta x_\parallel. \tag{38}$$

Eqs. (37)–(38) can be further simplified to obtain

$$\Delta x_\parallel = -\int_0^{\tilde{\chi}} d\chi\, (D+E_\parallel) - \frac{1+\tilde{z}}{H(\tilde{z})}\int_0^{\tilde{\chi}} d\chi\, (D'+E'_\parallel) \tag{39}$$

and

$$\begin{aligned}\Delta x^i_\perp = \tilde{\chi}\left(E^i{}_j\hat{\tilde{n}}^j - E_\parallel \hat{\tilde{n}}^i\right)_o \\ + \int_0^{\tilde{\chi}} d\chi \Big[-2\frac{\tilde{\chi}}{\chi}\left(E^i{}_j\hat{\tilde{n}}^j - E_\parallel\hat{\tilde{n}}^i\right) \\ + (\tilde{\chi}-\chi)\partial^i_\perp\left(D+E_\parallel\right)\Big].\end{aligned} \tag{40}$$

Note that the terms involving perturbations at the observer's location have dropped out of Eq. (39). This equation does not quite agree with Eq. (16) in [9], where $E_\parallel$ has the opposite sign in the first term. This difference also carries through to their Eq. (36). However, all these terms come from the metric pertburation $\delta g_{ij}\hat{\tilde{n}}^i\hat{\tilde{n}}^j$, hence they should always involve the combination $D+E_\parallel$. For the numerical results reported in [9, 10], this difference is of no relevance as they evaluate the power spectrum in conformal Newtonian gauge where $E=0$ [10].

C. Observed galaxy number density

The observed number of galaxies contained within a volume $\tilde{V}$ defined in terms of the observed coordinates is given by a (gauge-invariant) integral over a three-form

$$\begin{aligned}N &= \int_{\tilde{V}} \sqrt{-g(x^\alpha)}\, n_g(x^\alpha)\, \varepsilon_{\mu\nu\rho\sigma} u^\mu(x^\alpha) \frac{\partial x^\nu}{\partial\tilde{x}^1}\frac{\partial x^\rho}{\partial\tilde{x}^2}\frac{\partial x^\sigma}{\partial\tilde{x}^3} d^3\tilde{\mathbf{x}} \\ &= \int_{\tilde{V}} \sqrt{-g}\, n_g(x^\alpha)\, \frac{1}{a(x^0)}\varepsilon_{ijk}\frac{\partial x^i}{\partial\tilde{x}^1}\frac{\partial x^j}{\partial\tilde{x}^2}\frac{\partial x^k}{\partial\tilde{x}^3} d^3\tilde{\mathbf{x}} \\ &= \int_{\tilde{V}} \sqrt{-g}\, n_g(x^\alpha)\, \frac{1}{a(x^0)}\left|\frac{\partial x^i}{\partial\tilde{x}^j}\right| d^3\tilde{\mathbf{x}}.\end{aligned} \tag{41}$$

Here, $\mathbf{x}$ is given in terms of $\tilde{\mathbf{x}}$ by Eq. (36), $\varepsilon_{\mu\nu\rho\sigma}$ is the Levi-Civita tensor, and n_g is the physical number density of galaxies as a function of "true" comoving locations (in synchronous-comoving gauge). In the second line, we have adopted the synchronous-comoving gauge, where the oberver velocities reduce to $u^\mu = (1/a, 0, 0, 0)$. In this case, not surprisingly, the volume element reduces to the ordinary Jacobian $|\partial x^i/\partial\tilde{x}^j|$. Note that perturbations enter Eq. (41) in three places: through the determinant $\sqrt{-g}$; through the position- and redshift-dependence of the galaxy density n_g, and through the Jacobian $|\partial x^i/\partial\tilde{x}^j|$. This Jacobian is

$$\left|\frac{\partial x^i}{\partial\tilde{x}^j}\right| = \left|\delta^i_j + \frac{\partial\Delta x^i}{\partial\tilde{x}^j}\right| = 1 + \frac{\partial\Delta x^i}{\partial\tilde{x}^i}, \tag{42}$$

where we have worked to first order in the displacements $\Delta\mathbf{x}$. Furthermore, noting that $\sqrt{-\bar{g}} = a^4$, where $\bar{g}_{\mu\nu}$ is the background metric, we have

$$\sqrt{-g} = a^4\left(1 + \frac{1}{2}\delta g^\mu_\mu\right). \tag{43}$$

Finally, the galaxy density perturbations are usually measured with respect to the average density of galaxies at fixed observed redshift, $\bar{n}_g(\tilde{z})$. We assume that when averaged over the whole survey, $\langle\delta z\rangle = 0$ so that $\langle\tilde{z}\rangle = \bar{z}$ [Eq. (33)]. Also, in this paper, we follow common convention and define the galaxy density perturbations δ_g with respect to the *comoving* galaxy density. We thus have for the intrinsic comoving galaxy density

$$a^3(\bar{z}) n_g(\mathbf{x},\bar{z}) = a^3(\bar{z})\bar{n}_g(\bar{z})\,[1+\delta_g(\mathbf{x},\bar{z})], \tag{44}$$

where $\bar{z}$ again denotes the redshift that would have been observed in an unperturbed Universe, and δ_g denotes the intrinsic fluctuations in the comoving galaxy density. Using Eq. (33) and expanding to first order, we obtain

$$\begin{aligned}a^3(z) n_g(\mathbf{x},\bar{z}) = a^3(\tilde{z})\bar{n}_g(\tilde{z})\,[1+\delta_g(\tilde{\mathbf{x}})] \\ - (1+\tilde{z})\frac{d(a^3\bar{n}_g)}{dz}\Big|_{z=\tilde{z}}\delta z.\end{aligned} \tag{45}$$

Note that the distinction between $\delta_g(\tilde{\mathbf{x}})$ and $\delta_g(\mathbf{x})$ is second order (this effect, analogous to CMB lensing, can however become important for rapidly varying correlation functions [14]).

We can now expand Eq. (41). We define the *observed* galaxy density $\tilde{n}_g$ via

$$\int_{\tilde{V}} a^3(\tilde{z})\tilde{n}_g(\tilde{\mathbf{x}},\tilde{z}) d^3\tilde{\mathbf{x}} = N, \tag{46}$$

so that

$$\begin{aligned}a^3(\tilde{z})\tilde{n}_g(\tilde{\mathbf{x}},\tilde{z}) &= \sqrt{-g}\frac{1}{a}\, n_g(\mathbf{x},z)\left|\frac{\partial x^i}{\partial\tilde{x}^j}\right| \\ &= \left(1+\frac{1}{2}\delta g^\mu_\mu\right) a^3(\bar{z}) n_g(\mathbf{x},\bar{z})\left(1+\frac{\partial\Delta x^i}{\partial\tilde{x}^i}\right).\end{aligned} \tag{47}$$

For the Jacobian, we use Eq. (15) to obtain

$$\begin{aligned}\frac{\partial\Delta x^i}{\partial\tilde{x}^i} &= \partial_\parallel\Delta x_\parallel + \Delta x_\parallel\partial_i\hat{\tilde{n}}^i + \partial_{\perp\, i}\Delta x^i_\perp \\ &= \partial_\parallel\Delta x_\parallel + \frac{2\Delta x_\parallel}{\tilde{\chi}} - 2\hat{\kappa},\end{aligned} \tag{48}$$

where we have defined the coordinate convergence as

$$\hat{\kappa} \equiv -\frac{1}{2}\partial_{\perp\, i}\Delta x^i_\perp. \tag{49}$$

Note that the coordinate along $\hat{\tilde{\boldsymbol{n}}}$ is defined through the observed redshift $\tilde{z}$. Hence, $\partial_\parallel = (d\bar{\chi}/dz)\partial/\partial\tilde{z}$. Since the

derivative is applied to first-order displacements, it suffices to use the zeroth order expression $\partial_\parallel = \partial/\partial\chi|_{\chi=\tilde{\chi}}$.

Using Eq. (39) for $\Delta x_\parallel$, we obtain the first two terms in the Jacobian

$$\Delta x_\parallel = -\int_0^{\tilde{\chi}} d\chi (D + E_\parallel) - \frac{1+\tilde{z}}{H(\tilde{z})}\delta z \tag{50}$$

and

$$\begin{aligned}\partial_\parallel \Delta x_\parallel = & -(D+E_\parallel)\Big|_{\tilde{\chi}} - \frac{1}{H(\tilde{z})}\delta z \frac{d}{d\tilde{z}}\left[\frac{1+\tilde{z}}{H(\tilde{z})}\right] \\ & - \frac{1+\tilde{z}}{H(\tilde{z})}(D' + E'_\parallel).\end{aligned} \tag{51}$$

Using Eq. (40) we find for the convergence

$$\hat{\kappa} = \kappa + \frac{1}{2}\nabla_\perp^2 E + \frac{1}{\tilde{\chi}} E_{,i}(o)\hat{n}^i - \hat{n}^i E'_{,i}(o), \tag{52}$$

where

$$\kappa = -\frac{1}{2}\int_0^{\tilde{\chi}} d\chi\,(\tilde{\chi}-\chi)\,\frac{\chi}{\tilde{\chi}}\nabla_\perp^2\left(D - \frac{1}{3}\nabla^2 E - E''\right) \tag{53}$$

is the usual definition of the convergence in synchronous-comoving gauge and the derivatives of E with (o) are evaluated at the observer. The details of the derivation of $\hat{\kappa}$ can be found in App. B 2.

Finally, we can expand Eq. (47) to linear order in the perturbations:

$$\begin{aligned}\frac{\tilde{n}_g(\tilde{\mathbf{x}},\tilde{z})}{\bar{n}_g(\tilde{z})} &= 1 + 3D + \delta_g + b_e\delta z + \frac{2\Delta x_\parallel}{\tilde{\chi}} + \partial_\parallel \Delta x_\parallel - 2\hat{\kappa} \\ &= 1 + 2D - E_\parallel + \delta_g + b_e\delta z + \frac{2\Delta x_\parallel}{\tilde{\chi}} - 2\hat{\kappa} \\ &\quad - \left[1 - \frac{1+\tilde{z}}{H}\frac{dH(\tilde{z})}{d\tilde{z}}\right]\delta z - \frac{1+\tilde{z}}{H(\tilde{z})}(D' + E'_\parallel)\Big|_{\tilde{\chi}}.\end{aligned} \tag{54}$$

Here, $\delta\chi$ is given by Eq. (35), and δz is given by Eq. (31). Further, we have defined

$$b_e \equiv \frac{d\ln(a^3\bar{n}_g)}{d\ln a}\Big|_{\tilde{z}} = -\frac{1}{1+\tilde{z}}\frac{d\ln(a^3\bar{n}_g)}{dz}\Big|_{\tilde{z}}. \tag{55}$$

Throughout this section, we have neglected the magnification bias contribution. This will be discussed in Sec. II E.

D. Observed galaxy density contrast

In galaxy surveys, we calculate the galaxy density perturbations $\tilde{\delta}_g(\tilde{\mathbf{x}}) = \tilde{n}_g(\tilde{\mathbf{x}})/\langle\tilde{n}_g\rangle - 1$ by referring to the average number density $\langle\tilde{n}_g\rangle$ at *fixed observed redshift*. In this sense, we measure the galaxy density contrast in the uniform redshift gauge, where the constant-time hypersurface is defined by $\delta z = 0$. In the following, we assume that all fluctuations in n_g are due to large-scale structure, and ignore any contributions from e.g. varying survey depth and extinction. Using the result Eq. (54), we obtain

$$\begin{aligned}\tilde{\delta}_g(\tilde{\mathbf{x}}) = \delta_g &+ b_e\delta z - \frac{1+\tilde{z}}{H(\tilde{z})}\partial_\parallel^2 E' \\ &- \left(1 - \frac{1+\tilde{z}}{H}\frac{dH(\tilde{z})}{d\tilde{z}} + \frac{2}{\tilde{\chi}}\frac{1+\tilde{z}}{H(\tilde{z})}\right)\delta z + 2\phi \\ &- \frac{2}{\tilde{\chi}}[E' - E'(o)] - \frac{2}{\tilde{\chi}}\int_0^{\tilde{\chi}} d\chi\,(\phi + E'') - 2\kappa \\ &- \frac{1+\tilde{z}}{H(\tilde{z})}\phi' + 2\partial_\parallel E'(o),\end{aligned} \tag{56}$$

where $\phi \equiv D - \nabla^2 E/3$ (see App. B 3 for more details). In App. C, we apply Eq. (56) to analytical test cases where the exact result is known; these results serve as a cross-check of our result as well as to elucidate the significance of the various contributions. The terms in the first line contain the gauge-invariant intrinsic galaxy density perturbation (Sec. III) and the standard redshift-distortion contribution. The terms on the second line contain the change in volume entailed by the redshift perturbation. Finally, the last two lines contain further volume distortions from the metric at the source position, Doppler effect, time delay, and lensing convergence.

The observer terms in Eq. (56), $2\tilde{\chi}^{-1}E'(o)$ and $2\partial_\parallel E'(o)$, contribute only to the monopole and dipole of the galaxy distribution respectively. Therefore for most analyses that use the $\ell \geq 2$ multipoles of the galaxy distribution, or the small angle approximation, they can be neglected. The monopole term is not even measurable since we do not know the true mean galaxy density. (The dipole of a galaxy distribution *is* measurable in principle; indeed it has been used to search for e.g. inhomogeneous initial conditions [15].)

In App. D we connect this expression with the result for $\delta_{\rm obs}$ of [9]. Besides notational differences we clarify there, the most critical difference is that we obtain a term

$$\delta_g + b_e\delta z, \tag{57}$$

which takes into account the difference in the mean galaxy number density [Eq. (45)] between synchronous-comoving gauge and the uniform-redshift slicing, on which we measure the mean number density [the combination Eq. (57) is manifestly gauge invariant, as we shall show in the next section]. This term is not considered in Yoo et al. [9], as they relate the galaxy overdensity to the matter overdensity δ_m through the gauge-invariant relation

$$\delta_g = b(\delta_m - 3\delta z), \tag{58}$$

where $\delta_m(\mathbf{x}) = \rho_m(\mathbf{x})/\bar{\rho}_m - 1$ is the fractional matter overdensity defined in whichever gauge is adopted. Clearly, Eq. (58) is equivalent to assuming a linear bias relation in terms of density, $\delta_g = b\delta_m$, in the *uniform-redshift gauge*. We will discuss these issues in the next section.

On the other hand, by transforming Eq. (56) into conformal-Newtonian gauge, we are able to confirm that our result matches Eq. (30) in the recent paper by Challinor & Lewis [11]. This comparison is detailed in App. D as well.

E. Magnification bias

Equation (56) applies to the clustering of objects selected according to their intrinsic physical properties, their redshift, and their observed position on the sky. While one could in principle construct such a sample – e.g. a temperature-limited sample of X-ray clusters – most real samples in observational cosmology also depend on the apparent flux from the source. That is, they have a selection probability that depends on how the luminosity distance $D_{\rm L}$ differs from the mean luminosity distance $\bar{D}_{\rm L}(z)$. The sample selection may also depend on the angular size of the source, but this is not independent since the conservation of photon phase space density relates the angular diameter and luminosity distances[7]

$$D_{\rm L} = (1+\tilde{z})^2 D_{\rm A}. \tag{59}$$

This section evaluates the additional terms that would appear in Eq. (56) in the presence of a dependence on magnification. Such terms are however highly dependent on the galaxy sample and are not included in the numerical or graphical results displayed here. Their implications for realistic surveys on very large scales (and in particular how they differ from magnification effects in the small-scale limit) are left for a future paper.

The key parameter that we need to measure is the magnification

$$\mathcal{M} \equiv \frac{D_{\rm A}^{-2}}{\bar{D}_{\rm A}^{-2}(\tilde{z})} = \frac{D_{\rm L}^{-2}}{\bar{D}_{\rm L}^{-2}(\tilde{z})}, \tag{60}$$

which has mean value 1 and represents the perturbation to the solid angle or flux of a source, relative to a source at the same observed redshift $\tilde{z}$ in the unperturbed Universe. We may also write $\delta\mathcal{M} \equiv \mathcal{M} - 1$. The galaxy overdensity is then

$$\tilde{\delta}_g = \tilde{\delta}_g(\text{no mag}) + \mathcal{Q}\delta\mathcal{M}, \tag{61}$$

where $\tilde{\delta}_g$(no mag) is the overdensity computed from Eq. (56) and

$$\mathcal{Q} = \left.\frac{\partial \ln \tilde{n}_g}{\partial \ln \mathcal{M}}\right|_{\tilde{z}} \tag{62}$$

is the dependence of the observed number counts on magnification. For a magnitude-limited sample with cumulative luminosity function $\bar{n}(>L)$ we have $\mathcal{Q} = -d\ln\bar{n}(>L)/d\ln L$. A more general criterion, e.g. one that includes a "size" cut to reject stellar contamination [16], would have $\mathcal{Q}$ that must be determined by simulating the observations.

From Eq. (61) we see that we need only determine how $\delta\mathcal{M}$ depends on the metric perturbations in order to have a complete description of the magnification bias.

Fortunately, we have already constructed the key ingredients in evaluating $\mathcal{M}$. If we consider a right-handed 3-dimensional orthonormal basis $\{\hat{n}^i, \hat{\alpha}^i, \hat{\beta}^i\}$ where $\hat{n}^i$ is the direction of observation, then the angular diameter distance can be inferred from the area perpendicular to the line of sight spanned by the rays along the past light cone near $\hat{n}^i$,

$$D_A^2 = \sqrt{-g(x^\alpha)}\,\varepsilon_{\mu\nu\rho\sigma} u^\mu \hat{\ell}^\nu \frac{\partial x^\rho}{\partial \hat{n}^i}\frac{\partial x^\sigma}{\partial \hat{n}^j}\hat{\alpha}^i\hat{\beta}^j, \tag{63}$$

where the partial derivatives are taken at fixed $\tilde{\chi}$ and $\hat{\ell}^\mu$ is a unit purely spatial vector ($u_\mu\hat{\ell}^\mu = 0$) pointed away from the observer (in the sense that a photon emitted from the source with 4-velocity parallel to the null direction $u^\mu - \ell^\mu$ reaches the observer). Using the chain rule to replace the derivatives with those involving $\tilde{x}^i$ gives

$$\begin{aligned}\mathcal{M}^{-1} &= \frac{D_A^2}{[\bar{a}(\tilde{\chi})]^2\tilde{\chi}^2} \\ &= \frac{\sqrt{-g(x^\alpha)}}{[\bar{a}(\tilde{\chi})]^2}\,\varepsilon_{\mu\nu\rho\sigma}u^\mu\hat{\ell}^\nu\frac{\partial x^\rho}{\partial\tilde{x}^i}\frac{\partial x^\sigma}{\partial\tilde{x}^j}\hat{\alpha}^i\hat{\beta}^j.\end{aligned} \tag{64}$$

Next we observe that $\hat{\ell}^\nu$ is parallel to the spatial part of $L^\nu = \partial x^\nu/\partial\tilde{\chi}|_n$, since it is the spatial part of the tangent vector to the past light cone. Since $\hat{\ell}^\nu$ is a unit vector and L^ν is a past-directed null vector, it follows that

$$\hat{\ell}^\nu = \frac{L^\nu}{L^\sigma u_\sigma} + u^\nu; \tag{65}$$

using $u_\sigma = (-a,0,0,0)$ and $u^k = 0$ we find

$$\hat{\ell}^k = \frac{L^k}{a(x^0)\,L^0} = \frac{1}{a(x^0)}\frac{\partial x^k/\partial\tilde{\chi}}{-\partial x^0/\partial\tilde{\chi}}. \tag{66}$$

Using this and collapsing the Levi-Cevita symbol to 3 dimensions, we find

$$\mathcal{M}^{-1} = \frac{\sqrt{-g(x^\alpha)}}{-[\bar{a}(\tilde{\chi})a(x^0)]^2\partial x^0/\partial\tilde{\chi}}\varepsilon_{abc}\frac{\partial x^a}{\partial\tilde{x}^h}\frac{\partial x^b}{\partial\tilde{x}^i}\frac{\partial x^c}{\partial\tilde{x}^j}\hat{n}^h\hat{\alpha}^i\hat{\beta}^j. \tag{67}$$

Since $\{\hat{n}^i, \hat{\alpha}^i, \hat{\beta}^i\}$ form an orthonormal basis, we simplify this to

$$\mathcal{M}^{-1} = \frac{\sqrt{-g(x^\alpha)}}{-[\bar{a}(\tilde{\chi})a(x^0)]^2\partial x^0/\partial\tilde{\chi}}\left|\frac{\partial x^i}{\partial\tilde{x}^j}\right|. \tag{68}$$

Now we are in a position to compute the pieces of Eq. (68). We already know that $\sqrt{-g(x^\alpha)} = a^4(1+3D)$

[7] In the presence of opacity of intergalactic medium (IGM), e.g. due to Thomson scattering, this is not necessarily true. However, IGM opacity is a very small effect and we do not consider it in this paper.

and $|\partial x^i/\partial\tilde{x}^j| = 1 + \partial\Delta x^i/\partial\tilde{x}^i$ [the latter is given by Eq. (48)]. Finally the null condition gives

$$-\frac{dx^0}{d\tilde{\chi}} = (1 + D + E_\parallel)\frac{dx_\parallel}{d\tilde{\chi}} = 1 + D + E_\parallel + \partial_\parallel \Delta x_\parallel. \quad (69)$$

We thus find

$$\mathcal{M}^{-1} = \left[\frac{a(x^0)}{\bar{a}(\tilde{\chi})}\right]^2 \left(1 + 2D - E_\parallel + 2\frac{\Delta x_\parallel}{\tilde{\chi}} - 2\hat{\kappa}\right), \quad (70)$$

or

$$\delta\mathcal{M} = -2\delta z - 2D + E_\parallel - 2\frac{\Delta x_\parallel}{\tilde{\chi}} + 2\hat{\kappa}. \quad (71)$$

This makes sense: the perturbation to the magnification contains the obvious coordinate convergence term $2\hat{\kappa}$, but it also has three other pieces: a contribution $-2\Delta x_\parallel/\tilde{\chi}$ associated with bringing the source closer to or father from the observer; a contribution $2(-\delta z - D)$ associated with the isotropic conversion from coordinate distances to physical distances (itself having both a part from the change in scale factor at the source and the metric perturbation); and a part $E_\parallel$ associated with the anisotropy of the coordinate system (E_{ij} is traceless and magnification depends only on the perturbation to transverse distances).

Expanding $\Delta x_\parallel$ using Eq. (50) and $\hat{\kappa}$ using Eq. (52) gives an alternate expression

$$\begin{aligned}\delta\mathcal{M} &= -2\delta z - 2\phi - \frac{2}{\tilde{\chi}}[\partial_\parallel E - \partial_\parallel E(o)] + 2\kappa - 2\partial_\parallel E'(o) \\ &\quad + \frac{2}{\tilde{\chi}}\left[\int_0^{\tilde{\chi}} (D + E_\parallel) d\chi + \frac{1+\tilde{z}}{H(\tilde{z})}\delta z\right]. \end{aligned} \quad (72)$$

The integral may be simplified by replacing $D + E_\parallel \to \phi + \partial_\parallel^2 E$ and then doing a double integration by parts using Eq. (B26),

$$\begin{aligned}\delta\mathcal{M} &= -2\phi + \frac{2}{\tilde{\chi}}[E' - E'(o)] + 2\kappa - 2\partial_\parallel E'(o) \\ &\quad + \frac{2}{\tilde{\chi}}\int_0^{\tilde{\chi}} (\phi + E'') d\chi + \left[-2 + \frac{2}{\tilde{\chi}}\frac{1+\tilde{z}}{H(\tilde{z})}\right]\delta z. \end{aligned} \quad (73)$$

III. GALAXY BIAS IN A RELATIVISTIC CONTEXT

In order to make progress from Eq. (56), we need to relate the intrinsic galaxy overdensity δ_g (here written in synchronous-comoving gauge) to the matter and metric perturbations. Fortunately, since we are interested in large scales, we only need to consider terms linear in perturbations. What are the relevant quantities on which the physical galaxy density might depend?

The most important characteristics of the large-scale environment of a given galaxy are its mean density, and the evolutionary stage (proper time since the Big Bang, or linear growth factor). In fact, on sufficiently large scales, these are the only quantities of relevance to the galaxy two-point correlations [17] [8].

We can formalize this statement by considering some large spatial volume within the Universe centered around the spacetime point x_p^μ, on a constant-age hypersurface, $t_U =$ constant, where t_U denotes the proper time of comoving observers since the Big Bang. Then, the number of galaxies (or, more generally, tracers) within that volume can only depend on the enclosed mass M, and the age of the Universe in that volume t_U which is being kept fixed:

$$N_g = F(M;\, t_U;\, x_p^\mu). \quad (74)$$

Here, the explicit dependence on x_p^μ indicates any stochasticity in the relation between N_g and the local density and age. We now assume that the volume V is large enough so that linear perturbation theory applies. Then, in a given coordinate system $(\tau, \mathbf{x})$, the enclosed mass is given by

$$\begin{aligned} M &= \int_V \rho = \bar{\rho}_m(\tau)[1 + \delta\ln\rho]V \\ &= \bar{\rho}_m(\tau)[1 + \delta_m - 3aH\delta\tau]V. \end{aligned} \quad (75)$$

Here, $\bar{\rho}_m(\tau)$ is the average (physical) matter density in the background (equivalent to ρ averaged over the entire constant-coordinate-time hypersurface), while δ_m is the matter density perturbation on a *constant-coordinate-time* hypersurface. The second line follows from $\delta\ln\rho \equiv \rho/\bar{\rho}_m - 1$ and $d\ln\bar{\rho}_m/d\tau = -3aH$, and we have defined $-\delta\tau(\mathbf{x})$ to be the displacement in coordinate time corresponding to a $t_U =$ constant hypersurface:

$$a(\tau)[\tau - \delta\tau(\mathbf{x})] = t_U = \text{constant}. \quad (76)$$

Thus, the term $-3aH\delta\tau$ in Eq. (75) comes in from going from a constant-age hypersurface to a constant-coordinate-time hypersurface. Note that in Eq. (75) the perturbations are to be considered averaged over the volume V.

In exactly the same way, we can define the average (physical) galaxy number density $\bar{n}_g$ on constant-coordinate-time hypersurfaces. Then, the same reasoning leading to Eq. (75) leads to

$$\begin{aligned} N_g &= \int_V n_g = \bar{n}_g(\tau)[1 + \delta\ln n_g]V \\ &= \bar{n}_g(\tau)\left[1 + \delta_g + b_{ep}\, aH\delta\tau\right]V, \end{aligned} \quad (77)$$

where $b_{ep} = d\ln\bar{n}_g/d\ln a$. We can now equate this to our

[8] This assumes that there is no orientation-dependent selection of galaxies. Such a selection will introduce a dependence on the large-scale tidal field as well [18].

general ansatz Eq. (74),

$$\begin{aligned} N_g &= F(M;\, t_U;\, x_p^\mu) \\ &= \bar{F}(\bar{\rho}_m V; t_U)[1 + b(\delta_m - 3aH\delta\tau) + \varepsilon] \\ &= \bar{n}_g(\tau)\,[1 + \delta_g + b_{ep}\, aH\delta\tau]\, V. \end{aligned} \tag{78}$$

Here, we have defined $\bar{F}(M, t_U) \equiv \langle F(M, t_U, x_p^\mu)\rangle_{t_U}$, and introduced the bias

$$b \equiv \frac{\partial \ln \bar{F}(M; t_U)}{\partial \ln M}\Big|_{\bar{\rho}_m V} = \frac{\partial \ln \bar{F}(\rho_V V; t_U)}{\partial \ln \rho_V}\Big|_{\bar{\rho}_m} \tag{79}$$

and the stochastic contribution to galaxy density

$$\varepsilon(x^\mu) = \frac{F(M, t_U, x^\mu)}{\bar{F}(M, t_U)} - 1. \tag{80}$$

Also ρ_V denotes the average matter density (on the $t_U = $ const slice) within the volume V.

At first order, the bias b defined in this way is only a function of τ; and ε denotes the stochastic contribution to galaxy clustering, which at first order is only a function of the spacetime point (ε is here considered to be first order as well). In the background ($\delta_m \to 0, \delta\tau \to 0$), Eq. (78) implies, not surprisingly, $\bar{n}_g(\tau)V = \bar{F}(\bar{\rho}_m V; a\tau)$. To first order in the perturbations, recall that Eq. (78) must hold in *any* coordinate system. Thus, we conclude that the galaxy density perturbation is given in general by

$$\begin{aligned} \delta_g(x^\mu) = b(\tau)[\delta_m(x^\mu) - 3aH(\tau)\delta\tau(x^\mu)] \\ - b_{ep}(\tau)\, aH(\tau)\delta\tau(x^\mu) + \varepsilon(x^\mu). \end{aligned} \tag{81}$$

On sub-horizon scales, $aH\delta\tau$ becomes negligible compared to δ_m (for standard choices of gauge). Eq. (81) shows that in this limit we recover the usual bias relation $\delta_g = b\delta_m + \varepsilon$. Furthermore, if we choose synchronous gauge where all comoving observers are synchronized so that $t_U = a\tau$ everywhere and thus $\delta\tau = 0$, the linear bias relation holds on *all* scales. Note that the definition Eq. (79) is precisely what is commonly called a peak-background split bias parameter [19, 20].

This derivation was phrased in terms of the physical galaxy density. The reasoning and Eq. (81) trivially hold for the comoving galaxy density $a^3 n_g$ as well, the only difference being that δ_g is now the fractional perturbation in comoving number density, and b_{ep} is replaced with Eq. (55),

$$b_e = \frac{d\ln(a^3\bar{n}_g)}{d\ln a}.$$

From now on, we shall exclusively consider comoving number densities, as we did in Sec. II.

The bias relation Eq. (81) holds in all gauges, and the bias parameters b and b_e do not depend on the gauge choice. This is not very surprising, since the bias parameters defined here are in principle observable: b [Eq. (79)] quantifies the response of the galaxy number in a given volume at fixed age of the Universe to a change in the average mass density within this volume; b_e [Eq. (55)] quantifies the dependence of the average (background) number density of galaxies on the age of the Universe. To see the gauge-invariance of these bias parameters explicitly, consider the effect of a gauge transformation, specifically a change in the time coordinate,

$$\tau \to \check{\tau} = \tau + T, \tag{82}$$

where T can in general be a function of τ and $\mathbf{x}$ (spatial gauge transformations do not affect the density perturbations at linear order). By using Eq. (A3) in App. A, we find that δ_m and δ_g transform as

$$\begin{aligned} &\check{\delta}_m = \delta_m + 3aHT \;\text{ and} \\ &\check{\delta}_g = \delta_g - \frac{d\ln(a^3\bar{n}_g)}{d\tau}T = \delta_g - b_e\, aHT. \end{aligned} \tag{83}$$

On the other hand, ε is gauge-invariant. Note that a change in time coordinate (slicing) implies a change in the redshift perturbation δz [Eq. (33)] through

$$(1 + \check{z})\delta\check{z} = (1 + z)\delta z + HT, \tag{84}$$

with $d\bar{z}/d\tau = -H$.

The previous two equations clearly show that the combination $\delta_g + b_e\delta z$ appearing in Eq. (56) is gauge-invariant, independent of any bias relation. On the other hand, under the same gauge transformation with fixed b and b_e, Eq. (81) changes as

$$\begin{aligned} \check{\delta}_g &= b(\delta_m - 3aH\delta\tau) - b_e\, aH(\delta\tau + T) + \varepsilon \\ &= \delta_g - b_e\, aHT + \varepsilon, \end{aligned} \tag{85}$$

where we have used Eq. (55) in the second line. That is, we recover the gauge transformation of δ_g with fixed bias parameters, and, in this sense, the bias parameters defined through Eq. (79) and Eq. (55) are gauge-invariant.

We now see that a gauge-invariant expression for the galaxy number density [Eq. (56)], and a gauge-invariant definition of the galaxy bias are separate issues. In Refs. [9, 10, 13], the second issue was not addressed explicitly, and in Refs. [9, 10] b_e was implicitly set to zero.

A. Bias parameters from universal mass function approach

In this section, we show how both b and b_e can be estimated in the universal mass function approach. We adopt the synchronous-comoving gauge, which is implicit in the reasoning of this approach. The universal mass function approach is expected to be valid for objects selected via a proxy for halo mass; however if the selection criteria are sensitive to merger history (e.g. one selects active galactic nuclei) then the universal mass function may not be valid. This is analogous to the merger bias effect in models with primordial non-Gaussianity [2, 21].

In the simplest picture of galaxy biasing, one assumes that galaxies form inside density peaks in Lagrangian space whose height exceeds some critical matter density contrast δ_c. In regions with large-scale overdensity δ_l, this threshold is effectively lowered to $\delta_c - \delta_l$. If we denote the average abundance of tracers of mass M as $\bar{n}(M, \delta_c)$, the galaxy density contrast on large scales is then linearly related to the matter density contrast via

$$\delta_g(M;\delta_l) = \left(1 - \frac{\partial \ln \bar{n}(M,\delta_c,\tau)}{\partial \delta_c}\right)\delta_l = b\delta_l, \qquad (86)$$

if we truncate the Taylor expansion in linear order. The first term comes from mass conservation when transforming from Lagrangian to Eulerian space. As shown in the previous section, this argument is not in general correct in the context of general relativity. Note that if we were to choose a non-synchronous gauge (such as conformal-Newtonian or uniform-redshift gauge), peaks in different regions are at different evolutionary stages, so that the collapse threshold δ_c is not simply a constant. Therefore, the galaxy density contrast must also depend on the evolutionary stage, or age of the universe, in the region considered. However, in a synchronized gauge where $\delta\tau = 0$, the argument leading to Eq. (86) is applicable. Thus, Eq. (86) is a valid bias parameter which can be used in the correct, gauge-invariant bias expansion Eq. (81).

We can also obtain a useful analytical estimate for b_e, assuming that the abundance of galaxies follows a universal mass function,

$$\bar{n}(M) = \frac{\bar{\rho}_m}{M^2} f(\nu) \left|\frac{d\ln\sigma}{d\ln M}\right|. \qquad (87)$$

First, the linear density bias is given by [Eq. (86)]

$$b = 1 - \frac{\partial \ln \bar{n}}{\partial \delta_c} = 1 - \frac{d\ln f(\nu)}{d\nu}\frac{1}{\sigma}. \qquad (88)$$

On the other hand, b_e is given by

$$\begin{aligned} b_e &= \frac{\partial \ln(a^3\bar{n})}{\partial \ln a} = \frac{\partial \ln f(\nu)}{\partial \ln a} = \frac{d\ln f(\nu)}{d\nu}\frac{d\nu}{d\sigma}\frac{d\sigma}{d\ln a} \\ &= (1-b)\sigma\left(-\frac{\nu}{\sigma}\right)\sigma\frac{d\ln\sigma}{d\ln a}. \end{aligned} \qquad (89)$$

The logarithmic derivative of σ can be further simplified via linear perturbation theory as

$$\frac{d\ln\sigma}{d\ln a} = \frac{d\ln D}{d\ln a} \equiv f. \qquad (90)$$

Here $f \approx \Omega_{\rm m}^{0.6}$ is the usual logarithmic growth rate familiar from redshift-space distortion theory [22]. In summary, we obtain

$$b_e = (b-1)\sigma\nu f = \delta_c f(b-1). \qquad (91)$$

Note that the abundance of rarer, more strongly biased halos evolves faster (larger b_e), and that the overall rate is set by the growth rate f. Eq. (91) is useful for estimating the magnitude of the corrections to the galaxy power spectrum. Note however that the universal mass function prescription might not be a good description of actual tracers whose redshift evolution is influenced by non-gravitational physics (such as star formation, feedback, reionization, etc). The key point however is that for any given survey, b_e is in fact observable, if the redshift-dependence of the source selection function is known.

B. Bias in synchronous-comoving gauge

In the synchronous-comoving gauge assumed in our derivation in Sec. II, there is no perturbation to the 00-component of the metric. Moreover, the constant-time hypersurfaces are orthogonal to the velocities of comoving observers (in other words, $v = 0$). In this gauge, every comoving observers' proper time is synchronized, and all observers on a given τ =constant hypersurface are at the same evolutionary stage, which implies $\delta\tau = 0$. The density field in standard N-body simulations is also defined precisely in this gauge [23].

We now see that the gauge-invariant bias relation Eq. (81) is equivalent to the well-known linear bias relation between δ_g and δ_m in synchronous gauge,

$$\delta_g^{(\rm sc)} = b\delta_m^{(\rm sc)}, \qquad (92)$$

where the superscripts denote that the variables are defined in synchronous-comoving gauge. Inserting this into Eq. (56) then yields the observed galaxy overdensity, completely described by the metric and matter perturbations and two numbers specific to the tracer population: the linear bias b and the count slope with respect to redshift $d\ln(a^3\bar{n}_g)/dz$ (equivalent to b_e). Note that the latter parameter is observable in galaxy surveys, while the bias b is a parameter that needs to be fitted for.

IV. THE LARGE-SCALE GALAXY POWER SPECTRUM

We now calculate the observed galaxy power spectrum including the bias relation and the volume effect we have calculated in the previous sections. Throughout this section, we use the cosmological parameters from Table 1 ("WMAP+BAO+H_0 ML") of Komatsu et al. [24] as our reference cosmology. As explained in App. B 3, we neglect the lensing contribution κ, as it is not simply incorporated into a three-dimensional power spectrum. Further, we neglect two very small contributions, the integrated Sachs-Wolfe (ISW) contribution to δz, and the time-delay contribution $\propto \int d\chi\,(\phi + E'')/\tilde{\chi}$. We also neglect the stochastic contribution ε to δ_g in the following.

Neglecting the ISW contribution, we have (App. B 1)

$$\delta z(\tilde{\chi}) = \partial_\parallel E'(\tilde{\chi}) + E''(\tilde{\chi}), \qquad (93)$$

where we have dropped the unobservable, constant contribution from the perturbations evaluated at o. Using Eq. (56), Eq. (73), and the results from Sec. III, the observed galaxy density contrast written in terms of perturbations in synchronous-comoving gauge is then given by (see App. B for the derivation)

$$\tilde{\delta}_g = b\delta_m^{(\rm sc)} + b_e(\partial_\parallel E' + E'') + 2(1-\mathcal{Q})\phi - \frac{\partial_\parallel^2 E'}{aH} - \frac{2}{\tilde{\chi}}(1-\mathcal{Q})E' + (\mathcal{C}-1)(\partial_\parallel E' + E''), \quad (94)$$

where

$$\mathcal{C} = \frac{1+z}{H}\frac{dH}{dz} - \frac{1+z}{H}\frac{2}{\tilde{\chi}}(1-\mathcal{Q}) - 2\mathcal{Q}. \quad (95)$$

In a ΛCDM Universe, the first term in $\mathcal{C}$ can be simplified to yield

$$\mathcal{C} = \frac{3}{2}\Omega_m(z) - \frac{1+z}{H}\frac{2}{\tilde{\chi}}(1-\mathcal{Q}) - 2\mathcal{Q}. \quad (96)$$

where $\Omega_m(z)$ is the matter density parameter at redshift z. In Fourier space, Eq. (94) reads

$$\tilde{\delta}_g(\boldsymbol{k}) = b\delta_m^{(sc)} + b_e(ik\mu E' + E'') + 2(1-\mathcal{Q})\phi + \mu^2\frac{k^2E'}{aH} - (1-\mathcal{Q})\frac{2E'}{\tilde{\chi}} + (\mathcal{C}-1)(ik\mu E' + E''), \quad (97)$$

where μ is the cosine of wave-vector $\boldsymbol{k}$ with the line-of-sight direction.

Finally, by relating the synchronous-comoving gauge metric perturbations to the density contrast δ_m (App. A 3), we can further simplify $\tilde{\delta}_g$ as

$$\frac{\tilde{\delta}_g}{\delta_m} = b + f\mu^2 + \frac{\mathcal{A}}{x^2} + \frac{i\mu}{x}\mathcal{B}, \quad (98)$$

where $x \equiv k/aH$ is the wavenumber in units of the comoving horizon, $f \equiv d\ln D/d\ln a$, and we have defined the coefficients

$$\mathcal{A} = \frac{3}{2}\Omega_m\left[b_e\left(1 - \frac{2f}{3\Omega_m}\right) + 1 + \frac{2f}{\Omega_m} + \mathcal{C} - f - 2\mathcal{Q}\right] \quad (99)$$

and

$$\mathcal{B} = f\left[b_e + \mathcal{C} - 1\right]. \quad (100)$$

For given value of b_e and $\mathcal{Q}$, $\mathcal{A}$ and $\mathcal{B}$ are only functions of redshift, which incorporate the relativistic bias as well as the volume distortion and magnification effects. In principle, b_e can be measured from the survey itself provided one has good knowledge of the redshift-dependence of the selection function. In the following, we will use

$$b_e = \delta_{\rm c} f(b-1) \quad (101)$$

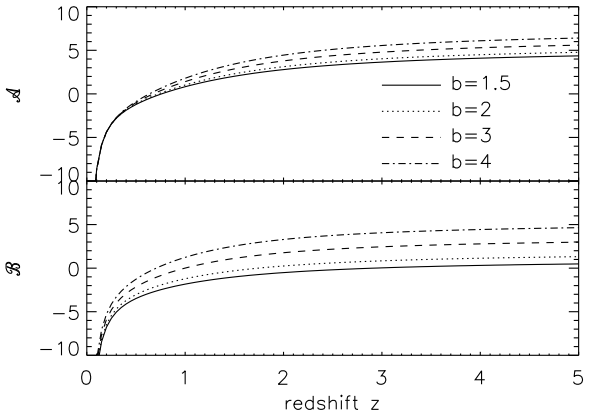

FIG. 2: Coefficients of new terms in observed galaxy overdensity in synchronous comoving gauge Eq. (98) introduced by relativistic volume effect and bias. Here, we plot for $b = 1.5$ (solid), $b = 2$ (dotted), $b = 3$ (dashed) and $b = 4$ (dot-dashed) cases, and b_e is calculated assuming the universality of the mass function [Eq. (91)]. We ignore the magnification effect by setting $\mathcal{Q} = 0$.

as predicted by the universal mass function ansatz [Sec. III A] for our illustrations. Figure 2 shows $\mathcal{A}$ and $\mathcal{B}$ as function of redshift when we only include relativistic volume and bias effect, i.e. $\mathcal{Q} = 0$. Note that both $\mathcal{A}$ and $\mathcal{B}$ diverge to $-\infty$ as $z \to 0$, because of the $1/\tilde{\chi}$ factor in $\mathcal{C}$ [Eq. (95)] which is a result of the volume distortion by velocities and gravitational redshifts. Figure 3 shows $\mathcal{A}$ and $\mathcal{B}$ for fixed bias ($b = 2$), and varying magnification ($\mathcal{Q} = -1$, 0.5, 1, and 2). Note that for the case of $\mathcal{Q} = 1$, which is the case for the diffuse source, magnification effect cancels volume distortion, and both $\mathcal{A}$ and $\mathcal{B}$ are small. For sufficiently high redshift when the Universe is approximately matter dominated, $\mathcal{C} \to 3\Omega_m/2 - 2\mathcal{Q} \simeq 1.5 - 2\mathcal{Q}$ and $f \to 1$, so that $b_e \to \delta_c(b-1)$ and we can approximate the coefficients as $\mathcal{A} \to 5.2 - 6\mathcal{Q} + \delta_c(b-1)/2$, $\mathcal{B} \to 0.5 - 2\mathcal{Q} + \delta_c(b-1)$.

Note that on small scales, when $x \gg 1$, we recover the usual Fourier-space galaxy overdensity in "Newtonian theory",

$$\tilde{\delta}_g \overset{x\gg 1}{=} (b + f\mu^2)\delta_m. \quad (102)$$

From Eq. (98) we can calculate the observed galaxy power spectrum in terms of the linear matter power spectrum $P^{(\rm sc)}(k)$ in synchronous comoving gauge, yielding

$$\frac{P_g(k,\mu)}{P^{(\rm sc)}(k)} = (b+f\mu^2)^2 + 2(b+f\mu^2)\frac{\mathcal{A}}{x^2} + \frac{\mathcal{A}^2}{x^4} + \frac{\mu^2\mathcal{B}^2}{x^2}. \quad (103)$$

Note again that we have neglected all projected quantities here, most importantly the magnification contribution -2κ. Furthermore, the flat-sky calculation employed here is likely not applicable to the very largest scales in

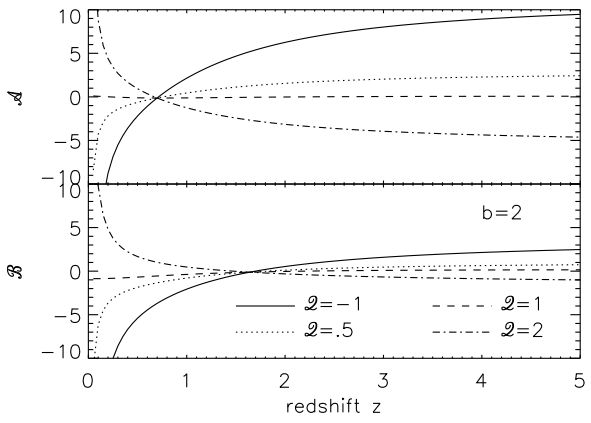

FIG. 3: Same as Fig. 2, but for fixed bias ($b = 2$) and varying magnification with $\mathcal{Q} = -1$ (solid), 0.5 (dotted), 1 (dashed), 2 (dot-dashed). For the diffuse sources, $\mathcal{Q} = -1$, magnification effect cancels almost all volume effects, and, therefore, relativistic effect becomes smaller.

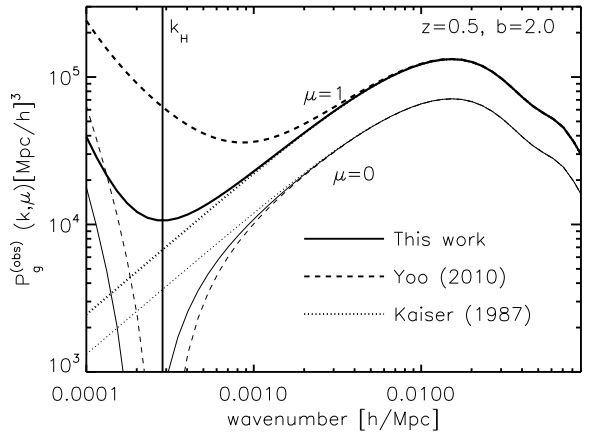

FIG. 4: Three different theoretical predictions of observed galaxy power spectrum on large scales for galaxies with linear bias $b = 2$ at redshift $z = 0.5$, and assuming $\mathcal{Q} = 0$: Newtonian linear theory [22] (dotted line), relativistic linear theory with linear bias in uniform redshift gauge [9] (dashed line), and relativistic linear theory with linear bias in synchronous comoving gauge (this work, solid line). We show both line-of-sight directional power spectrum ($\mu = 1$, thick lines) and perpendicular directional power spectrum ($\mu = 0$, thin lines). The vertical solid line indicates $k = aH$ at $z = 0.5$.

actual galaxy surveys. Here we are mainly interested in the issue of galaxy biasing however, and defer the calculation of the full angular galaxy power spectrum to future work.

Fig. 4 shows the galaxy power spectrum in three different calculations, each for $\mu = 0$ and $\mu = 1$. The dotted lines show the linear small-scale limit given by the Kaiser formula. The solid lines show the relativistic calculation Eq. (103) using the galaxy bias prescription derived in Sec. III, i.e. a linear bias relation in synchronous-comoving gauge. Clearly, the prediction departs from the Kaiser formula on scales $k \lesssim 10^{-3}\,h/\mathrm{Mpc}$. The dashed lines in Fig. 4 show the result of [9] for comparison. As we have seen in Sec. III, their result is equivalent to linear biasing in the uniform-redshift gauge. We see that the departures from the small-scale limit are much more significant in this latter calculation, showing that the precise choice of bias relation is important on very large scales.

Fig. 5 shows the two-dimensional galaxy power spectrum from Eq. (103), illustrating the evolution of the angular dependence of $P_g(k,\mu)$ with scale. Also shown for comparison is the prediction of the Kaiser formula [22]. Again, deviations appear for $k \lesssim 10^{-3}\,h/\mathrm{Mpc}$ and become more significant for transverse separations.

A. Effective primordial non-Gaussianity

Our results show that the observed power spectrum departs from the small-scale calculation on sufficiently large scales, with terms proportional to $(k/aH)^{-2}$ and $(k/aH)^{-4}$. This is reminiscent of the scale-dependent bias induced by primordial non-Gaussianity [1]. It is thus natural to compare the two effects. Neglecting all relativistic effects, and redshift distortion terms that are unimportant on large scales [25], the observed galaxy power spectrum for local primordial non-Gaussianity is given by

$$\frac{P_g^{(\mathrm{NG})}(k)}{P^{(\mathrm{sc})}(k)} = (b + \Delta b(k) + f\mu^2)^2 = (b + f\mu^2)^2 + 2\Delta b(k)(b + f\mu^2) + \Delta b^2(k). \quad (104)$$

Here we have defined the bias correction

$$\Delta b(k) = \frac{2 f_{\mathrm{NL}}(b-1)\delta_{\mathrm{c}}\, 3\Omega_{m0}H_0^2}{2D(z)k^2T(k)} = f_{\mathrm{NL}}\delta_{\mathrm{c}}(b-1)\frac{3\Omega_m(z)H^2a^3}{D(z)k^2T(k)} \simeq \frac{3}{2x^2}\Omega_m(z)\delta_{\mathrm{c}}(b-1)f_{\mathrm{NL}}\frac{2a}{D(z)}, \quad (105)$$

where in the last line we have assumed that $k \lesssim 0.01\,h/\mathrm{Mpc}$ so that $T(k) = 1$. We can define an effective non-linearity parameter $f_{\mathrm{NL}}^{\mathrm{eff}}$ such that the scale-dependent non-Gaussian bias inserted into the small-scale expression Eq. (104) leads to a power spectrum matching the actual observed power spectrum in the Gaussian case including the relativistic effects. However the relativistic corrections affect modes perpendicular and parallel to the line of sight differently, while the non-Gaussian scale-dependent bias is isotropic. [Note in particular the $\mathcal{B}$ term in Eq. (103).] Therefore, we can, in principle, distinguish the relativistic effect from the non-Gaussian scale dependent bias through the angular

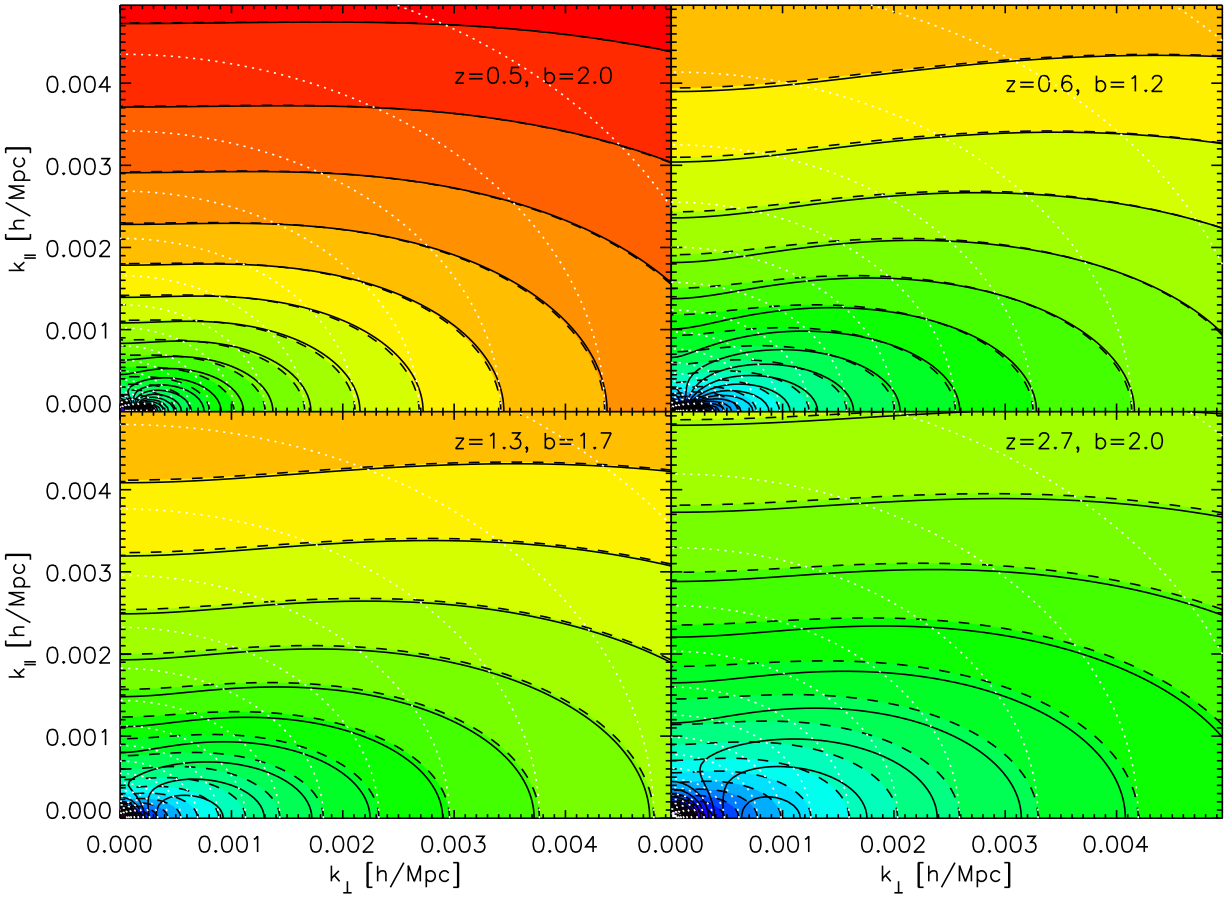

FIG. 5: Observed galaxy power spectrum (Eq. (103)) as function of $k_\parallel$ and $k_\perp$. The color contours and dashed lines show the Newtonian result from Kaiser [22], while the solid lines show the result including relativistic corrections. Here we have set $\mathcal{Q} = 0$. For reference, we also show the real space power spectrum contours as white dotted lines.

dependence of the 2D power spectrum. Given the limited number of modes on scales $k \lesssim 10^{-3}h/\mathrm{Mpc}$, it is more realistic to consider the effect on the angle-averaged power spectrum monopole

$$P_g^{(\ell=0)}(k) = \frac{1}{2}\int_{-1}^{1} d\mu\, P_g(k,\mu). \tag{106}$$

From Eq. (103), we find that the monopole power spectrum becomes

$$\frac{P_g^{(\ell=0)}(k) - P_g^{(\mathrm{Kaiser},\ell=0)}(k)}{P^{(\mathrm{sc})}(k)} = \left[2\left(b+\frac{f}{3}\right)\mathcal{A} + \frac{\mathcal{B}^2}{3}\right]\frac{1}{x^2} + \frac{\mathcal{A}^2}{x^4}, \tag{107}$$

and from Eq. (104), we find that

$$\frac{P_g^{(\mathrm{NG},\ell=0)}(k) - P_g^{(\mathrm{Kaiser},\ell=0)}(k)}{P^{(\mathrm{sc})}(k)} = \frac{3}{x^2}\Omega_m\delta_c(b-1)f_{\mathrm{NL}}\frac{2a}{D(z)}\left[b+\frac{f}{3}\right] + \Delta b^2(k), \tag{108}$$

where

$$P_g^{(\mathrm{Kaiser},\ell=0)}(k) = \left[b^2 + \frac{2}{3}bf + \frac{1}{5}f^2\right]P_m^{(\mathrm{sc})}(k) \tag{109}$$

is the monopole galaxy power spectrum given by the Kaiser formula. By equating the term proportional to x^{-2} in Eq. (107) and Eq. (108), we find the effective

non-linearity parameter as

$$f_{\rm NL}^{\rm eff} = \frac{D(a)}{a}\frac{1}{6\Omega_m\delta_c(b-1)}\left[2\mathcal{A}+\frac{\mathcal{B}^2}{3b+f}\right]$$
$$= \frac{1}{2}\frac{D(a)}{a}\Bigg[f\left(1-\frac{2f}{3\Omega_m}\right) + \frac{1+2f/\Omega_m+\mathcal{C}-f-2\mathcal{Q}}{\delta_c(b-1)} + \frac{\delta_c(b-1)}{3\Omega_m(3b+f)}\left(f^2+f\frac{\mathcal{C}-1}{\delta_c(b-1)}\right)^2\Bigg]. \quad (110)$$

Fig. 6 shows the monopole of the galaxy power spectrum, using the full expression Eq. (103) and Eq. (104) with Eq. (110). They generally agree very well, apart from the lowest-redshift case.

The effective $f_{\rm NL}$ given by Eq. (110) can serve as a useful tool to forecast for a given survey whether relativistic effects become important: if a survey achieves a forecasted precision on the local $f_{\rm NL}$ of order $f_{\rm NL}^{\rm eff}$, then relativistic effects are relevant. Fig. 7 shows $f_{\rm NL}^{\rm eff}$ for differently biased tracers as a function of redshift when $\mathcal{Q}=0$. Typical values are around 0.2, and generally lower than 0.5. Note that we have assumed the universal mass function approach to estimate $f_{\rm NL}^{\rm eff}$; if for some reason the tracer number density evolves very rapidly with redshift so that $d\ln(a^3\bar{n}_g)/dz$ becomes large, $f_{\rm NL}^{\rm eff}$ would increase correspondingly. In general however, we expect that number to remain less than 1. The $f_{\rm NL}^{\rm eff}$ sharply rises around $z\sim 0$, because of $1/\tilde{\chi}$ factor in $\mathcal{C}$ [Eq. (95)]. Fig. 8 shows $f_{\rm NL}^{\rm eff}$ for galaxies of bias $b=2$ with different luminosity function with slope of ($\mathcal{Q}=-1$, 0.5, 1, 2). This figure indicates that $f_{\rm NL}^{\rm eff}$ varies greatly for different luminosity function, but does not exceed 2 except for low redshifts where, again, $f_{\rm NL}^{\rm eff}$ diverges due to $1/\tilde{\chi}$. This divergence however, is removed completely for the diffuse sources where $\mathcal{Q}=1$ (dashed line).

V. CONCLUSIONS

Future galaxy surveys will measure the clustering of galaxies on scales approaching the horizon. Thus, it is necessary to embed the observed galaxy density in a relativistic context. This problem has received considerable attention recently. In this paper, we have derived the observed galaxy density contrast $\tilde{\delta}_g$ in terms of the intrinsic galaxy overdensity δ_g and metric perturbations in the synchronous-comoving gauge (Sec. II). By transforming to conformal-Newtonian gauge, we reach agreement with the results of Refs. [11, 13]. On the other hand, we find some minor disagreement with the expression of Ref. [9], which can be traced back to a sign issue. In App. C, we also show that our formula for $\tilde{\delta}_g$ reproduces the correct analytic result for the following six test cases: (1) a pure spatial gauge mode, (2) a zero-wavenumber gauge mode, (3) a perturbation to the expansion history, (4) a small spatial curvature, (5) an anisotropic expansion history (Bianchi I cosmology), and (6) a potential-only mode in E that has no metric perturbations but leads to boundary terms at the observer. These tests use all of the terms in Eq. (56), and attaining agreement with the analytical results often involves delicate cancellations or combinations of various terms; thus they lend credibility to Eq. (56) and suggest that it is free of sign errors or similar issues.

One necessary, further ingredient for a description of galaxy clustering on large scales is a physical, gauge-invariant definition of galaxy bias. We present a straightforward physically motivated definition in Sec. III. This bias relation is easily seen to reduce to the standard linear bias relation in synchronous coordinates, where constant-time hypersurfaces coincide with constant-age hypersurfaces. The bias relation Eq. (81) can be seen as a proper generalization of the peak-background split bias. Using this result, we arrive at a simple expression for the observed galaxy density perturbations in synchronous-comoving gauge [Eq. (94)], described by the (gauge-invariant) bias parameter b, and the redshift evolution of the tracer population [through b_e, Eq. (55)].

The recent study of Baldauf et al. [26] has also reached the same conclusion by constructing locally flat spacetime coordinates around a freely-falling observer, where long-wavelength modes locally act as curvature. In that coordinate system, the galaxy number density is modulated not only by the local curvature but also the time difference between global time and local time whose effect exactly coincides to our b_e in Eq. (81). In contrast, Ref. [9] adopted a bias relation in the constant-observed-redshift gauge, which leads to considerably different predictions for the large-scale galaxy power spectrum. However, this does not seem to be a physical description of galaxy bias, since the age of the Universe is *not* constant on constant-observed-redshift slices.

In the picture outlined in Sec. III, it is also straightforward to understand the effect of primordial non-Gaussianity. Consider a constant-age hypersurface as defined in Sec. III, at some early time long before the tracers of interest formed. Since the linear growth factor is the same everywhere on this slice, the variance of the small-scale density field σ_R^2 smoothed on some scale R is also the same everywhere, in the case of Gaussian initial conditions. In the presence of non-Gaussianity of the local type, mode-coupling induces a modulation of σ_R^2 by long-wavelength (Bardeen) potential perturbations Φ_L, so that, within a region on a $t_U=$ const hypersurface where Φ_L can be considered constant, it is given by

$$\hat{\sigma}_R^2 = \sigma_R^2(1+4f_{\rm NL}\Phi_L). \quad (111)$$

Here, σ_R^2 is the variance derived from the Gaussian part of ϕ. We see that this is closely related to perturbing the local age of the Universe, which leads to a change in the local σ_R^2 as well. The relation between Φ and δ_m in

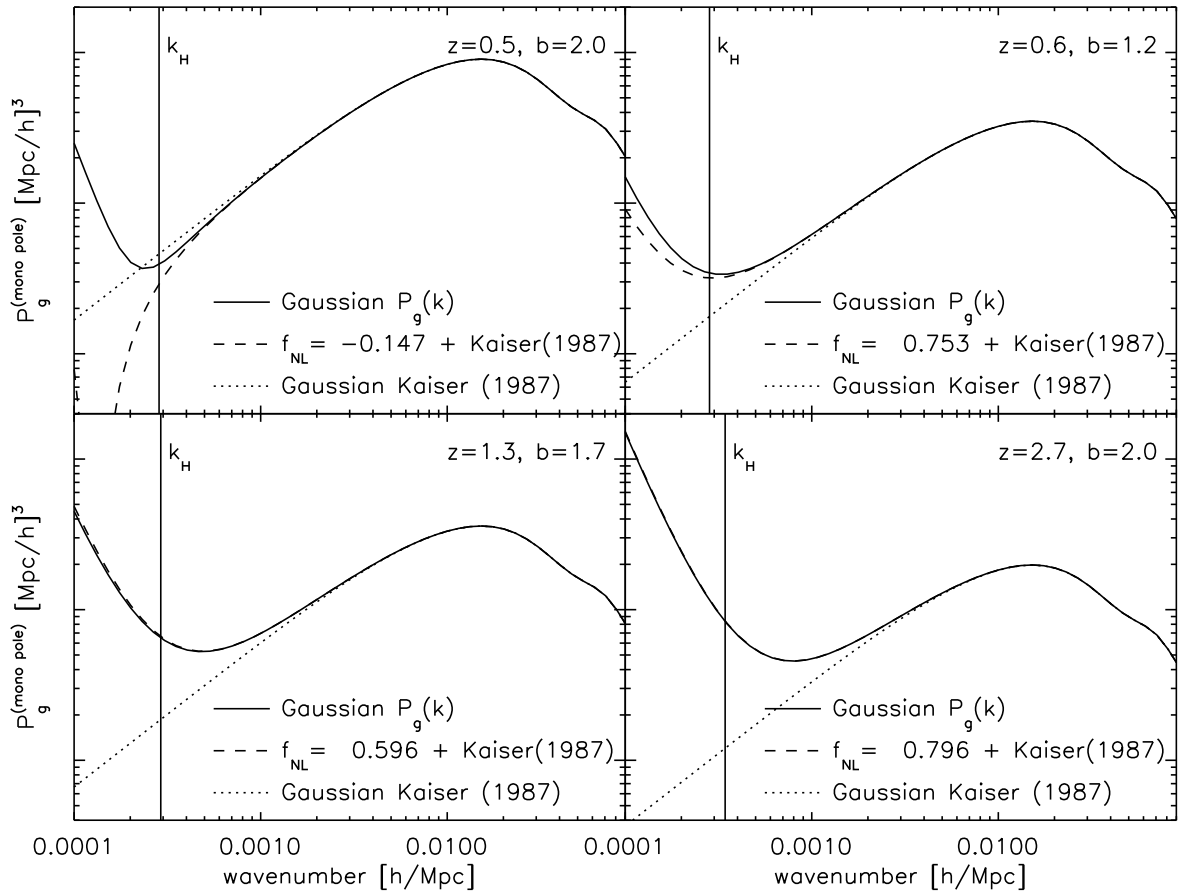

FIG. 6: Monopole galaxy power spectrum [Eq. (106)] from the full expression Eq. (103), and using the effective $f_{\rm NL}$ approximation, Eq. (104). We use the same set of bias and redshift as in Fig. 5 (and $\mathcal{Q}=0$). The effective $f_{\rm NL}$ approximation is valid within the horizon ($k \lesssim 1/aH$), marked by a vertical line, while it breaks down on large scales where the x^{-4} term in Eq. (107) is important. The breakdown is more apparent when $\mathcal{B}$ is large (upper two panels).

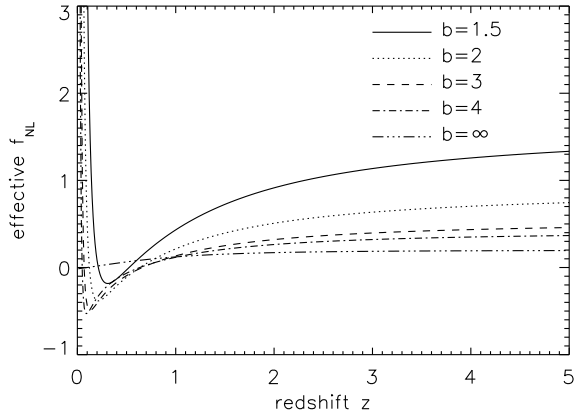

FIG. 7: Effective $f_{\rm NL}$ [Eq. (110)] as a function of redshift for different galaxy biases when $\mathcal{Q}=0$.

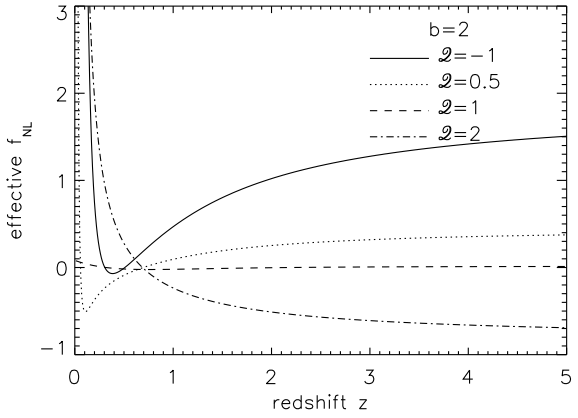

FIG. 8: Same as Fig. 7, but for galaxy bias ($b=2$) with different magnification $\mathcal{Q}=-1$, 0.5, 1 and 2.

synchronous-comoving gauge is given by (e.g., [27])

$$\delta_m^{(\rm sc)}(k,z) = \mathcal{M}(k,z)\Phi(k,z_*) = \frac{3\Omega_m H_0^2 k^2(1+z)}{2T(k)D(z)}\Phi(k,z_*), \quad (112)$$

where z_* is some reference redshift where the non-Gaussian parameter $f_{\rm NL}$ is defined (for example, that of the last-scattering surface). Using the universal mass function prescription (Sec. III A), we then see that the bias relation Eq. (81) in synchronous-comoving gauge is modified to

$$\delta_g^{(\rm sc)} = \left[b + 2f_{\rm NL}(b-1)\delta_c\mathcal{M}^{-1}(k)\right]\delta_m^{(\rm sc)}, \quad (113)$$

in agreement with [1]. It is straightforward to generalize this derivation to more general types of non-Gaussianity [27, 28]. Note in particular that (for the local case), the scale-dependent correction to $\delta_g^{(\rm sc)}$ is proportional to k^{-2} out to arbitrarily large scales (see also [12, 29]). Of course, on large scales it is necessary to include the other terms contributing to the observed $\tilde{\delta}_g$ in Eq. (94). We believe these results together with other recent work [11, 13, 26] allow us to unambiguously predict the two-point statistics of large-scale structure tracers on large scales.

Acknowledgments

We would like to thank Olivier Doré and the participants of the Michigan non-Gaussianity workshop for helpful discussions. DJ and FS are supported by the Gordon and Betty Moore Foundation at Caltech. CH is supported by the US National Science Foundation (AST-0807337), the US Department of Energy (DE-FG03-02-ER40701), and the David and Lucile Packard Foundation.

Appendix A: Metric variables and gauge transformations

Let us consider a general scalar coordinate transformation (T, L)

$$x^\alpha \to \check{x}^\alpha = x^\alpha + \left(T(x^\alpha), \partial^i L(x^\alpha)\right). \quad (A1)$$

While true scalar quantities are invariant under such a coordinate change, perturbations around the background do change because the background is time-dependent.

For example, consider a scalar function $\zeta(\tau,\mathbf{x})$ whose background value only depends on time $\bar{\zeta}(\tau)$. This is the case for all scalar functions in the homogeneous universe. As a scalar, the function ζ does not change under the coordinate transformation in Eq. (A1), and it is only background time τ, thus $\bar{\zeta}(\tau)$, that is changed. From the relation

$$\zeta = \bar{\zeta}(\tau) + \delta\zeta(\tau,\mathbf{x}) = \bar{\zeta}(\check{\tau}) + \check{\delta\zeta}(\check{\tau},\check{\mathbf{x}}), \quad (A2)$$

we calculate the scalar perturbation $\check{\delta\zeta}$ in the transformed coordinate in terms of the variables in the old coordinate as

$$\check{\delta\zeta} = \delta\zeta + \bar{\zeta}(\tau) - \bar{\zeta}(\tau+T) = \delta\zeta - \frac{d\bar{\zeta}(\tau)}{d\tau}T \quad (A3)$$

up to linear order in perturbations. By appyling Eq. (A3), we find that the matter density contrast and redshift perturbation transform as

$$\check{\delta}_m = \delta_m - \frac{d\ln\rho_m}{d\tau}T = \delta_m + 3aHT,$$
$$\check{\delta z} = \delta z + aHT, \quad \text{and}$$
$$\check{\delta}_g = \delta_g - b_e aHT, \quad (A4)$$

where in the second line we have used that $d\bar{z}/d\tau = -aH$. Hence, the quantity $\delta_m - 3\delta z$ remains invariant under gauge transformations. The scalar component of the peculiar velocity, $\partial_i v \equiv a dx^i/dt$, transforms as

$$\check{v} = v + L'. \quad (A5)$$

We can calculate the gauge transformation of higher rank vectors/tensors in a similar way, by applying the appropriate transformation law of the object.

1. General scalar metric perturbations

Consider a general FRW metric with scalar perturbations defined through

$$ds^2 = -a^2(1+2A)d\tau^2 - 2a^2 B_{,i}d\tau dx^i + a^2\left[(1+2D)\delta_{ij} + 2E_{ij}\right]dx^i dx^j \quad (A6)$$

where

$$E_{ij} = \left(\partial_i\partial_j - \frac{1}{3}\delta_{ij}\nabla^2\right)E. \quad (A7)$$

Then the metric perturbations transform as follows:

$$\check{A} = A - aHT - T',$$
$$\check{B} = B + L' - T,$$
$$\check{D} - \frac{1}{3}\nabla^2\check{E} = D - \frac{1}{3}\nabla^2 E - aHT, \quad \text{and}$$
$$\check{E} = E - L. \quad (A8)$$

Similarly, when the perturbed metric is defined through

$$ds^2 = -a^2(1+2\alpha)d\tau^2 - 2a^2\beta_{,i}d\tau dx^i + a^2\left[(1+2\varphi)\delta_{ij} + 2\gamma_{,ij}\right]dx^i dx^j, \quad (A9)$$

perturbations transform as follows:

$$\check{\alpha} = \alpha - aHT - T',$$
$$\check{\beta} = \beta + L' - T,$$
$$\check{\varphi} = \varphi - aHT, \quad \text{and}$$
$$\check{\gamma} = \gamma - L. \quad (A10)$$

Note that the spatial metric components in Eq. (A6) and Eq. (A9) are related through

$$\alpha = A \quad \text{and} \quad \varphi = D - \frac{1}{3}\nabla^2 E. \tag{A11}$$

2. From synchronous comoving to conformal Newtonian gauge

The two most commonly considered gauges in cosmology are the conformal-Newtonian gauge, which is defined through

$$B = E = 0 \quad \Leftrightarrow \quad \beta = \gamma = 0, \tag{A12}$$

using the convention Eq. (A6) and Eq. (A9), respectively, and the synchronous-comoving gauge, defined through

$$A = B = v = 0 \quad \Leftrightarrow \quad \alpha = \beta = v = 0, \tag{A13}$$

in the same conventions. Here we explicitly give the transformation between these two gauges, using the general expressions of the previous section. We find that

$$\begin{aligned} 0 &= \alpha - aHT - T', \\ 0 &= L' - T, \\ D - \frac{1}{3}\nabla^2 E &= \varphi - aHT, \\ E &= -L, \quad \text{and} \\ 0 &= v + L' \end{aligned} \tag{A14}$$

Solving these equations leads to the transformation from conformal-Newtonian to synchronous-comoving gauge,

$$D = \varphi + \frac{1}{3}\nabla^2 \int d\tau v + aHv \quad \text{and} \quad E = \int d\tau v, \tag{A15}$$

and the corresponding inverse transformation,

$$\begin{aligned} \alpha &= -aHE' - E'', \\ \varphi &= D - \frac{1}{3}\nabla^2 E - aHE', \quad \text{and} \\ v &= E'. \end{aligned} \tag{A16}$$

Note that in Eq. (A15), we have the freedom to add an integration constant, which reflects that D and E in synchronous gauge contain a spatial gauge mode. Such a gauge mode can be removed by introducing $\phi \equiv D - \nabla^2 E/3$ and taking time derivative of E. For example, Eq. (A16) contains only ϕ and E', because the conformal-Newtonian gauge has no residual gauge freedom.

3. Metric variables in synchronous gauge

In this appendix, we show the relation among three common parametrizations of synchronous-comoving gauge, and how to relate all metric perturbations to the matter density perturbation in the adiabatic case.

The convention used in this paper is

$$\delta g_{ij}(\tau, \mathbf{x}) = a^2(\tau)\left[2D(\tau, \mathbf{x})\delta_{ij} + 2E_{ij}(\tau, \mathbf{x})\right], \tag{A17}$$

where E_{ij} is defined to be traceless and related to the scalar $E(\tau, \mathbf{x})$ via

$$E_{ij}(\tau, \mathbf{x}) = \left(\partial_i\partial_j - \frac{1}{3}\delta_{ij}\nabla^2\right) E(\tau, \mathbf{x}) \tag{A18}$$

(see Bardeen [30]). In Yoo [10], the spatial metric perturbation is defined as

$$\delta g_{ij}(\tau, \mathbf{x}) = a^2(\tau)\left[2\phi(\tau, \mathbf{x})\delta_{ij} + 2\partial_i\partial_j\gamma(\tau, \mathbf{x})\right]. \tag{A19}$$

Comparing Eqs. (A17,A19), we find the relations

$$\phi(\tau, \mathbf{x}) = D(\tau, \mathbf{x}) - \frac{1}{3}\nabla^2 E(\tau, \mathbf{x}) \text{ and } \gamma(\tau, \mathbf{x}) = E(\tau, \mathbf{x}). \tag{A20}$$

In Fourier space, the metric in Eq. (A17) becomes

$$\begin{aligned} \delta g_{ij}(\tau, \mathbf{k}) \;=\; & a^2(\tau)\Big[2D(\tau, \mathbf{k})\delta_{ij} \\ & -2\left(\mathbf{k}_i\mathbf{k}_j - \frac{1}{3}k^2\delta_{ij}\right) E(\tau, \mathbf{k})\Big], \end{aligned} \tag{A21}$$

which can be compared with the spatial metric perturbations defined in Ma & Bertschinger [31]:

$$\begin{aligned} \delta g_{ij}(\boldsymbol{k}, \tau) = a^2(\tau)\Big[& \frac{\boldsymbol{k}_i\boldsymbol{k}_j}{k^2} h(\boldsymbol{k}, \tau) \\ & + 6\left(\frac{\boldsymbol{k}_i\boldsymbol{k}_j}{k^2} - \frac{1}{3}\delta_{ij}\right)\eta(\boldsymbol{k}, \tau)\Big]. \end{aligned} \tag{A22}$$

Comparing Eq. (A21) and Eq. (A22) leads to

$$D(\tau, \mathbf{k}) = \frac{h(\tau, \mathbf{k})}{6} \quad \text{and} \quad E(\tau, \mathbf{k}) = -\frac{h(\tau, \mathbf{k}) + 6\eta(\tau, \mathbf{k})}{2k^2}, \tag{A23}$$

and combining above results yields

$$\phi(\tau, \mathbf{k}) = -\eta(\tau, \mathbf{k}) \quad \text{and} \quad \gamma(\tau, \mathbf{k}) = -\frac{h(\tau, \mathbf{k}) + 6\eta(\tau, \mathbf{k})}{2k^2}. \tag{A24}$$

Now we relate the metric variables to the matter density contrast in synchronous gauge. First, let us consider the time derivative of E. The continuity equation in synchronous comoving gauge is given by [31]

$$\delta'_m(\tau, \mathbf{k}) = -\frac{1}{2}h'(\tau, \mathbf{k}), \tag{A25}$$

and from the Einstein equations we have [e.g. Eq. (22) of [31]]

$$k^2\eta'(\tau, \mathbf{k}) = 4i\pi G a^2 k^j \delta T^0_j \propto v = 0. \tag{A26}$$

Therefore, we calculate the time derivative of E as

$$E'(\tau, \mathbf{k}) = -\frac{h'(\tau, \mathbf{k})}{2k^2} = \frac{\delta'_m(\tau, \mathbf{k})}{k^2} = \frac{aHf}{k^2}\delta_m(\tau, \mathbf{k}), \tag{A27}$$

where $f = d\ln D/d\ln a$. From here, we can also calculate the second derivative of E as

$$E''(\tau,\mathbf{k}) = \frac{1}{k^2}\frac{\partial\left[aHf\delta_m(\tau,\mathbf{k})\right]}{\partial\tau} = \frac{1}{k^2}a^2H^2\left[\frac{3}{2}\Omega_m - f\right]\delta_m(\tau,\mathbf{k}), \tag{A28}$$

where the second equality comes from the time evolution of the linear density contrast (continuity and Euler equations). Finally, from the Einstein equation [Eq. (21a) in Ref. [31]], we calculate $\phi(\tau,\mathbf{k}) = -\eta(\tau,\mathbf{k})$ as

$$\begin{aligned}\phi(\tau,\mathbf{k}) =& -\frac{1}{2k^2}\left[aHh'(\tau,\mathbf{k}) + 8\pi Ga^2\delta T^0_0\right]\\ =& (a^2H^2f + 4\pi G\bar{\rho}_m a^2)\frac{\delta_m(\tau,\mathbf{k})}{k^2}\\ =& a^2H^2\left(f+\frac{3}{2}\Omega_m\right)\frac{\delta_m(\tau,\mathbf{k})}{k^2}.\end{aligned} \tag{A29}$$

Note that while D contains a spatial gauge mode, $\phi \equiv D - \nabla^2E/3$ does not contain any. Also, from Eq. (A26), it is obvious that ϕ is constant in time. The physical interpretation is that for a plane wave perturbation, two neighboring test particles separated by an infinitesimal distance perpendicular to $\mathbf{k}$ have a separation that is proportional to the background $a(t)$; only the component of separation parallel to $\mathbf{k}$ is perturbed.

Appendix B: Derivation of Eq. (94)

This section outlines the derivation of Eq. (94) from the expression for $\tilde{\delta}_g$ [Eq. (56)]. We begin by deriving a compact expression for δz, before moving on to the convergence $\hat{\kappa}$ and the derivation of Eq. (94).

1. Integrated Sachs-Wolfe term in synchronous comoving gauge

In this section, we show to identify the ISW term in synchronous-comoving gauge and derive a simplified expression for δz. In conformal Newtonian gauge, the ISW term is given by

$$\delta z_{\rm ISW} = -\int_0^{\tilde{\chi}} d\chi(\Phi+\Psi)', \tag{B1}$$

where Ψ and Φ are Bardeen's potential and prime denotes a derivative with respect to the conformal time τ. In synchronous comoving gauge, they are

$$\begin{aligned}\Psi =& -aHE' - E'' \quad \text{and}\\ \Phi =& -D + \frac{1}{3}\nabla^2E + aHE',\end{aligned} \tag{B2}$$

and the ISW term becomes

$$\delta z_{\rm ISW} = \int_0^{\tilde{\chi}} d\chi\left(D' - \frac{1}{3}\nabla^2E' + E'''\right). \tag{B3}$$

Using Eq. (31) and the definition of E, we find that the redshift perturbation in the same gauge is given by

$$\delta z = \int_0^{\tilde{\chi}} d\chi\left(D - \frac{1}{3}\nabla^2E + \partial_\parallel^2E\right)'. \tag{B4}$$

Now, we use that $\partial_\chi = \partial_\parallel - \partial_\tau$, and rewrite the redshift perturbation by successively applying integration by part:

$$\begin{aligned}\delta z =& \int_0^{\tilde{\chi}} d\chi\left[D' - \frac{1}{3}\nabla^2E' + (\partial_\chi+\partial_\tau)\,\partial_\parallel E'\right]\\ =& \left[\partial_\parallel E'\right]^s_o + \int_0^{\tilde{\chi}} d\chi\left[D' - \frac{1}{3}\nabla^2E' + (\partial_\chi+\partial_\tau)\,E''\right]\\ =& \left[\partial_\parallel E' + E''\right]^s_o + \int_0^{\tilde{\chi}} d\chi\left(D' - \frac{1}{3}\nabla^2E' + E'''\right).\end{aligned} \tag{B5}$$

The second, integral term is clearly equal to the ISW contribution, and neglecting it we obtain $\delta z = [\partial_\parallel E' + E'']^s_o$, which in Fourier space becomes

$$\delta z = ik\mu E' + E''. \tag{B6}$$

Here, we have ignored the contribution from the origin, and μ denotes the directional cosine between the wave vector and the line of sight direction.

2. Convergence in synchronous comoving gauge

In this section, we calculate the coordinate convergence in the synchronous comoving gauge defined in Eq. (49). By applying the perpendicular derivative $\partial_{\perp i}$ to the perpendicular directional displacement $\Delta x^i_\perp$ in Eq. (40), we find

$$\begin{aligned}\hat{\kappa} =& -\frac{1}{2}\nabla^2_\perp\int_0^{\tilde{\chi}} d\chi(\tilde{\chi}-\chi)\frac{\tilde{\chi}}{\chi}\left(D+E_\parallel\right)\\ &+\partial_{\perp\,i}\int_0^{\tilde{\chi}} d\chi\frac{\tilde{\chi}}{\chi}\left(E^i_j\hat{\tilde{n}}^j - E_\parallel\hat{\tilde{n}}^i\right)\\ &-\frac{1}{2}\partial_{\perp i}\left\{\tilde{\chi}[E_{ij}(o)\hat{n}^j - E_{jk}(o)\hat{n}^i\hat{n}^j\hat{n}^k]\right\}\\ \equiv& \hat{\kappa}^{(1)} + \hat{\kappa}^{(2)} + \hat{\kappa}^{(3)},\end{aligned} \tag{B7}$$

where we have labelled the three terms and used "(o)" to denote metric shear evaluated at the observer. In the first term, we have pulled out the perpendicular derivative inside the integral over the unperturbed geodesic. Hence the additional factor of $\tilde{\chi}/\chi$ in the integrand.

We begin with the $\hat{\kappa}^{(1)}$ term:

$$\begin{aligned}\hat{\kappa}^{(1)} =& -\frac{1}{2}\nabla^2_\perp\int_0^{\tilde{\chi}} d\chi(\tilde{\chi}-\chi)\frac{\tilde{\chi}}{\chi}\left(D - \frac{1}{3}\nabla^2E + \partial_\parallel^2E\right)\\ =& \kappa - \frac{1}{2}\nabla^2_\perp\int_0^{\tilde{\chi}} d\chi(\tilde{\chi}-\chi)\frac{\tilde{\chi}}{\chi}(\partial_\parallel^2E - E'').\end{aligned} \tag{B8}$$

This allows us to relate $\hat{\kappa}$ to κ with the introduction of some new terms. We can combine these terms with terms in $\hat{\kappa}^{(2)}$ if we simplify the latter: using the commutation relations Eqs. (9)–(13), we have

$$\begin{aligned}
&\hat{\hat{n}}^j E^i_j - \hat{\hat{n}}^i E_\parallel \\
&\quad = \hat{\hat{n}}^j \left(\partial_j \partial^i - \frac{1}{3}\delta^i_j \nabla^2\right) E - \hat{\hat{n}}^i \left(\partial_\parallel^2 - \frac{1}{3}\nabla^2\right) E \\
&\quad = \left(\hat{\hat{n}}^j \partial_j \partial^i - \hat{\hat{n}}^i \partial_\parallel^2\right) E = \left(\partial_\parallel \partial^i - \partial_\parallel \hat{\hat{n}}^i \partial_\parallel\right) E \\
&\quad = \partial_\parallel \partial^i_\perp E = \partial^i_\perp \partial_\parallel E - \frac{1}{\chi}\partial^i_\perp E, \qquad \text{(B9)}
\end{aligned}$$

and so

$$\hat{\kappa}^{(2)} = \nabla^2_\perp \int_0^{\tilde{\chi}} d\chi \left(\frac{\tilde{\chi}^2}{\chi^2}\partial_\parallel E - \frac{\tilde{\chi}^2}{\chi^3} E\right). \qquad \text{(B10)}$$

(Note again the additional factor of $\tilde{\chi}/\chi$ that arises since when we move $\partial^i_\perp$ outside the integral it acts at radius $\tilde{\chi}$ rather than χ.) Combining these gives

$$\begin{aligned}
\hat{\kappa}^{(1)} + \hat{\kappa}^{(2)} &= \kappa + \frac{1}{2}\nabla^2_\perp \int_0^{\tilde{\chi}} d\chi \Big[\Big(-\frac{\tilde{\chi}^2}{\chi} + \tilde{\chi}\Big)(\partial_\parallel^2 E - E'') \\
&\quad + 2\frac{\tilde{\chi}^2}{\chi^2}\partial_\parallel E - 2\frac{\tilde{\chi}^2}{\chi^3} E\Big] \\
&= \kappa + \frac{1}{2}\nabla^2_\perp \int_0^{\tilde{\chi}} d\chi \\
&\quad \times \Big[\Big(-\frac{\tilde{\chi}^2}{\chi} + \tilde{\chi}\Big)\frac{d}{d\chi}\left(2\partial_\parallel E - \frac{dE}{d\chi}\right) \\
&\quad + 2\frac{\tilde{\chi}^2}{\chi^2}\partial_\parallel E - 2\frac{\tilde{\chi}^2}{\chi^3} E\Big], \qquad \text{(B11)}
\end{aligned}$$

where in the second line we have used $' = \partial_\parallel - d/d\chi$. The $\partial_\parallel E$ terms form a total derivative, which may be separately evaluated:

$$\begin{aligned}
\hat{\kappa}^{(1)} + \hat{\kappa}^{(2)} &= \kappa + \frac{1}{2}\nabla^2_\perp \int_\epsilon^{\tilde{\chi}} d\chi \Big[\Big(\frac{\tilde{\chi}^2}{\chi} - \tilde{\chi}\Big)\frac{d^2E}{d\chi^2} - 2\frac{\tilde{\chi}^2}{\chi^3}E\Big] \\
&\quad + \nabla^2_\perp \left\{\Big(-\frac{\tilde{\chi}^2}{\chi} + \tilde{\chi}\Big)\partial_\parallel E\Big|_\epsilon^{\tilde{\chi}}\right\}. \qquad \text{(B12)}
\end{aligned}$$

The quantity in braces vanishes at $\tilde{\chi}$, whereas at $\epsilon \to 0$ it blows up. For this reason, we will evaluate this expression only for $\epsilon > 0$ and then take the limit after all divergences are cancelled. If we Taylor expand $\partial_\parallel E$ to order ϵ, we find

$$\partial_\parallel E(\epsilon) = \hat{n}^i E_{,i}(o) + \hat{n}^i\hat{n}^j \epsilon E_{,ij}(o) - \hat{n}^i E'_{,i}(o)\epsilon + \mathcal{O}(\epsilon^2). \qquad \text{(B13)}$$

The quantity in braces is then (keeping terms that are nonvanishing as $\epsilon \to 0^+$)

$$-\left(-\frac{\tilde{\chi}^2}{\epsilon} + \tilde{\chi}\right) E_{,i}(o)\hat{n}^i + \tilde{\chi}^2 \hat{n}^i\hat{n}^j E_{,ij}(o) - \tilde{\chi}^2 \hat{n}^i E'_{,i}(o). \qquad \text{(B14)}$$

The $\nabla^2_\perp$ operator pulls down a factor of 0 for monopoles, $-2/\tilde{\chi}^2$ for dipoles, and $-6/\tilde{\chi}^2$ for quadrupoles. It follows that

$$\begin{aligned}
\hat{\kappa}^{(1)} + \hat{\kappa}^{(2)} &= \kappa + \frac{1}{2}\nabla^2_\perp \int_\epsilon^{\tilde{\chi}} d\chi \Big[\Big(\frac{\tilde{\chi}^2}{\chi} - \tilde{\chi}\Big)\frac{d^2E}{d\chi^2} - 2\frac{\tilde{\chi}^2}{\chi^3}E\Big] \\
&\quad + \left(-\frac{2}{\epsilon} + \frac{2}{\tilde{\chi}}\right) E_{,i}(o)\hat{n}^i - 6E_{ij}(o)\hat{n}^i\hat{n}^j \\
&\quad + 2\hat{n}^i E'_{,i}(o). \qquad \text{(B15)}
\end{aligned}$$

The remaining integral is also a total derivative, although in this case two integrations by parts are necessary. Both terms can be integrated by parts to obtain a single derivative dE/dx; the integrals cancel leaving only the boundary terms:

$$\begin{aligned}
\hat{\kappa}^{(1)} + \hat{\kappa}^{(2)} &= \kappa + \frac{1}{2}\nabla^2_\perp \Big[\Big(\frac{\tilde{\chi}^2}{\chi} - \tilde{\chi}\Big)\frac{dE}{d\chi}\Big|_\epsilon^{\tilde{\chi}} + \frac{\tilde{\chi}^2}{\chi^2}E\Big|_\epsilon^{\tilde{\chi}}\Big] \\
&\quad + \left(-\frac{2}{\epsilon} + \frac{2}{\tilde{\chi}}\right) E_{,i}(o)\hat{n}^i - 6E_{ij}(o)\hat{n}^i\hat{n}^j \\
&\quad + 2\hat{n}^i E'_{,i}(o). \qquad \text{(B16)}
\end{aligned}$$

This simplifies to

$$\begin{aligned}
\hat{\kappa}^{(1)} + \hat{\kappa}^{(2)} &= \kappa + \frac{1}{2}\nabla^2_\perp \Big[-\left(\frac{\tilde{\chi}^2}{\epsilon} - \tilde{\chi}\right)\frac{dE}{d\chi}(\epsilon) - \frac{\tilde{\chi}^2}{\epsilon^2}E(\epsilon)\Big] \\
&\quad + \frac{1}{2}\nabla^2_\perp E + \left(-\frac{2}{\epsilon} + \frac{2}{\tilde{\chi}}\right) E_{,i}(o)\hat{n}^i \\
&\quad - 6E_{ij}(o)\hat{n}^i\hat{n}^j + 2\hat{n}^i E'_{,i}(o), \qquad \text{(B17)}
\end{aligned}$$

where $\nabla^2_\perp$ is evaluated at radius $\tilde{\chi}$.

Further simplification requires the limiting forms of the terms in Eq. (B17). A lowest-order expansion gives the quantity in brackets as

$$\begin{aligned}
&-\left(\frac{\tilde{\chi}^2}{\epsilon} - \tilde{\chi}\right)[\hat{n}^i E_i(o) - E'(o) + \epsilon\hat{n}^i\hat{n}^j E_{ij}(o) \\
&\quad - 2\epsilon\hat{n}^i E'_{,i}(o) + \epsilon E''(o)] \\
&-\frac{\tilde{\chi}^2}{\epsilon^2}[E(o) + \epsilon\hat{n}^i E_{,i}(o) - \epsilon E'(o) \\
&\quad + \frac{1}{2}\epsilon^2\hat{n}^i\hat{n}^j E_{,ij}(o) - \epsilon^2\hat{n}^i E'_{,i}(o) + \frac{1}{2}\epsilon^2 E''(o)]. \qquad \text{(B18)}
\end{aligned}$$

Again using that $\nabla^2_\perp$ operator pulls down a factor of 0 for monopoles, $-2/\tilde{\chi}^2$ for dipoles, and $-6/\tilde{\chi}^2$ for quadrupoles, we find that Eq. (B17) simplifies to

$$\begin{aligned}
\hat{\kappa}^{(1)} + \hat{\kappa}^{(2)} &= \kappa + \frac{1}{2}\nabla^2_\perp E + \frac{1}{\tilde{\chi}}E_{,i}(o)\hat{n}^i \\
&\quad - \frac{3}{2}E_{ij}(o)\hat{n}^i\hat{n}^j - \hat{n}^i E'_{,i}(o). \qquad \text{(B19)}
\end{aligned}$$

The third term, $\hat{\kappa}^{(3)}$, is independent of $\tilde{\chi}$ since it is a derivative of a quantity that depends linearly on $\tilde{\chi}$; hence

we may evaluate it on the unit sphere $\tilde{\chi} = 1$. We find

$$\begin{aligned}\hat{\kappa}^{(3)} &= -\frac{1}{2}E_{ij}(o)(\delta_{ij} - \hat{n}^i\hat{n}^j) + \frac{1}{2}E_{jk}(o)\big[2\hat{n}^j\hat{n}^k \\ &\quad +(\delta_{ij} - \hat{n}^i\hat{n}^j)\hat{n}^i\hat{n}^k + (\delta_{ik} - \hat{n}^i\hat{n}^k)\hat{n}^i\hat{n}^j\big] \\ &= \frac{3}{2}E_{ij}(o)\hat{n}^i\hat{n}^j. \end{aligned} \tag{B20}$$

Combining with Eq. (B19) gives

$$\hat{\kappa} = \kappa + \frac{1}{2}\nabla_\perp^2 E + \frac{1}{\tilde{\chi}}E_{,i}(o)\hat{n}^i - \hat{n}^i E'_{,i}(o). \tag{B21}$$

This is Eq. (52).

3. From Eq. (54) to Eq. (56) and Eq. (94)

Let us start from Eq. (54),

$$\begin{aligned}\tilde{\delta}_g(\tilde{\mathbf{x}}) &= \delta_g + b_e\delta z + 2D - E_\parallel \\ &\quad + 2\frac{\Delta x_\parallel}{\tilde{\chi}} - 2\hat{\kappa} - \left(1 - \frac{1+\tilde{z}}{H}\frac{dH(\tilde{z})}{d\tilde{z}}\right)\delta z \\ &\quad - \frac{1+\tilde{z}}{H(\tilde{z})}(D' + E'_\parallel)\Big|_{\tilde{\chi}}, \end{aligned} \tag{B22}$$

where

$$\Delta x_\parallel = -\int_0^{\tilde{\chi}} d\chi(D + E_\parallel) - \frac{1+\tilde{z}}{H(\tilde{z})}\delta z \tag{B23}$$

and we use Eq. (B21) for $\hat{\kappa}$. Also, in the previous section, we found that the redshift perturbation, ignoring the ISW term, is given by

$$\delta z = \partial_\parallel E' + E''. \tag{B24}$$

As shown in App. A 2, D and E contain spatial gauge modes, while $\phi \equiv D - \nabla^2 E/3$ and E' remove such gauge modes. We now collect the four terms in Eq. (B22) which contain gauge modes:

$$\begin{aligned}&2D - E_\parallel + 2\frac{\Delta x_\parallel}{\tilde{\chi}} - 2\hat{\kappa} \\ &= 2\phi + \frac{2}{3}\nabla^2 E - \left(\partial_\parallel^2 - \frac{1}{3}\nabla^2\right)E - \frac{2}{\tilde{\chi}}\int_0^{\tilde{\chi}} d\chi(D + E_\parallel) \\ &\quad - \frac{2}{\tilde{\chi}}\frac{1+\tilde{z}}{H(\tilde{z})}\delta z - 2\kappa - \nabla_\perp^2 E - \frac{2}{\tilde{\chi}}\hat{n}^i E_{,i}(o) + 2\hat{n}^i E'_{,i}(o) \\ &= 2\phi + \frac{2}{\tilde{\chi}}[\partial_\parallel E - \partial_\parallel E(o)] - \frac{2}{\tilde{\chi}}\int_0^{\tilde{\chi}} d\chi(\phi + \partial_\parallel^2 E) \\ &\quad - \frac{2}{\tilde{\chi}}\frac{1+\tilde{z}}{H(\tilde{z})}\delta z - 2\kappa + 2\partial_\parallel E'(o). \end{aligned} \tag{B25}$$

The third term can be further simplified by double integration by parts to yield

$$\begin{aligned}\int_0^{\tilde{\chi}} d\chi(\phi + \partial_\parallel^2 E) &= \int_0^{\tilde{\chi}} d\chi(\phi + E'') + E' + \partial_\parallel E \\ &\quad -E'(o) - \partial_\parallel E(o), \end{aligned} \tag{B26}$$

Then we find for the observed galaxy density contrast

$$\begin{aligned}\tilde{\delta}_g(\tilde{\mathbf{x}}) &= \delta_g + b_e\delta z - \frac{1+\tilde{z}}{H(\tilde{z})}\partial_\parallel^2 E' \\ &\quad - \left[1 - \frac{1+\tilde{z}}{H}\frac{dH(\tilde{z})}{d\tilde{z}} + \frac{2}{\tilde{\chi}}\frac{1+\tilde{z}}{H(\tilde{z})}\right]\delta z + 2\phi \\ &\quad - \frac{2}{\tilde{\chi}}[E' - E'(o)] - \frac{1+\tilde{z}}{H(\tilde{z})}\phi' - \frac{2}{\tilde{\chi}}\int_0^{\tilde{\chi}} d\chi\,(\phi + E'') \\ &\quad - 2\kappa + 2\partial_\parallel E'(o). \end{aligned} \tag{B27}$$

This is Eq. (56). Note that the magnification bias contribution $\mathcal{Q}\,\delta\mathcal{M}$ does not contain gauge modes [Eq. (73)].

To proceed to Eq. (94), we drop several terms:

- The observer terms (which contribute only to the monopole and dipole).
- The ϕ' term, since the $0i$ component of the Einstein equation ensures that in a ΛCDM universe $\phi' = 0$ [see Eq. (A26) and note that $\eta = -\phi$].
- The terms $-\frac{2}{\tilde{\chi}}\int_0^{\tilde{\chi}} d\chi(\phi + E'')$ in Eq. (56) and Eq. (73), corresponding to the time delay which is very small [14, 32].
- The terms involving the convergence κ, which is generally *not* small but is a projected quantity, and in the flat-sky limit contributes only to transverse modes.

Substituting in Eq. (B24) for δz and using Eq. (73) then yields Eq. (94). Conversion to Fourier space in the flat-sky limit – i.e. where we make the replacement $\partial_\parallel \to ik\mu$ – then gives Eq. (97).

Appendix C: Test cases for the observed galaxy overdensity

This appendix considers several analytical test cases that serve as a cross-check of Eq. (56). The first two cases are pure gauge modes, with the expected result that $\tilde{\delta}_g$ does not receive any contributions from such perturbations. We then consider a perturbed expansion history, spatial curvature, and a Bianchi type I cosmology with anisotropic expansion. Finally we consider a model with a time-dependent linear gradient in E, which has no metric perturbation but leads to a delicate cancellation of terms in the galaxy density. In all cases, the linearized version of the exact result can be derived straightforwardly, and we show that it agrees with the prediction of Eq. (56) in all cases. We further evaluate the magnification $\mathcal{M}$ using Eq. (73) and show that it matches the expected results.

1. Pure spatial gauge mode

The residual gauge freedom of the synchronous gauge allows us to reparameterize the spatial coordinates ac-

cording to $x^i \to x^i + \xi^i$, where ξ^i depends only on the spatial coordinates and not x^0. This leads to a spatial metric perturbation $h_{ij} = -a^2(\xi^i{}_{,j} + \xi^j{}_{,i})$. Since here we consider scalar perturbations only, ξ^i should be derived from a potential $\xi^i = \xi_{,i}$. If we start from an unperturbed Universe, the resulting metric perturbation is

$$D = -\frac{1}{3}\nabla^2\xi \quad \text{and} \quad E = -\xi. \tag{C1}$$

Eq. (C1) corresponds to a pure gauge mode.

For this mode, we proceed to evaluate δz, ϕ, and κ. Since D and E are time-independent, it is trivially seen that $\delta z = 0$, and Eq. (C1) immediately implies $\phi = 0$. Finally, since $D = \frac{1}{3}\nabla^2 E$ and $E'' = 0$ we can also see that $\kappa = 0$. Then Eq. (56) reduces to

$$\tilde{\delta}_g(\tilde{\mathbf{x}}) = \delta_g, \tag{C2}$$

which is the expected answer. That is, in this case we do not have any contributions to the galaxy density aside from the intrinsic contribution.

We may also evaluate the magnification using Eq. (73). With $E' = 0$ everywhere and $\delta z = \phi = \kappa = 0$, it is trivially seen that $\delta\mathcal{M} = 0$.

2. Zero-wavenumber gauge mode

There is another spatial gauge mode that does not fall into the rubric of Eq. (C1): the zero-wavenumber mode given by

$$D = \Xi + g_i x^i \quad \text{and} \quad E = 0, \tag{C3}$$

where Ξ is a constant scalar and $\mathbf{g}$ is a constant vector field. This is generated by the gauge perturbation

$$\xi^i = -\Xi x^i + \frac{1}{2}g^i|\mathbf{x}|^2 - g_j x^j x^i. \tag{C4}$$

Again we trivially have $\delta z = 0$, but this time $\phi = \Xi + \chi\mathbf{g}\cdot\hat{\mathbf{n}}$. Also we have

$$\nabla_\perp^2 D = \nabla_\perp^2(\chi\mathbf{g}\cdot\hat{\mathbf{n}}) = \frac{-2}{\chi}\mathbf{g}\cdot\hat{\mathbf{n}}, \tag{C5}$$

since $\mathbf{g}\cdot\hat{\mathbf{n}}$ is a dipole ($\ell = 1$) and for a pure multipole of order ℓ the operator $\nabla_\perp^2$ yields a factor of $-\ell(\ell+1)/\chi^2$. Thus we find

$$\kappa = -\frac{1}{2}\int_0^{\tilde{\chi}} d\chi(\tilde{\chi} - \chi)\frac{\chi}{\tilde{\chi}}\frac{-2}{\chi}\mathbf{g}\cdot\hat{\mathbf{n}} = \frac{1}{2}\tilde{\chi}\mathbf{g}\cdot\hat{\mathbf{n}}. \tag{C6}$$

The galaxy density perturbation obtained via Eq. (56) has only four nontrivial terms:

$$\tilde{\delta}_g = \delta_g + 2(\Xi + \tilde{\chi}\mathbf{g}\cdot\hat{\mathbf{n}}) - \frac{2}{\tilde{\chi}}\int_0^{\tilde{\chi}}(\Xi + \chi\mathbf{g}\cdot\hat{\mathbf{n}})\,d\chi - \tilde{\chi}\mathbf{g}\cdot\hat{\mathbf{n}}. \tag{C7}$$

Here the second term comes from the $+2\phi$ term in Eq. (56), the third term is the line of sight integral of $\phi + E'' = \phi$, and the last term comes from the -2κ. It is easily seen that these three terms cancel, leaving $\tilde{\delta}_g = \delta_g$, which is the expected answer.

Unlike the previous case, here the magnification contains nontrivial terms: substituting the nonzero values of ϕ and κ into Eq. (73), we find

$$\delta\mathcal{M} = -2(\Xi + \tilde{\chi}\mathbf{g}\cdot\hat{\mathbf{n}}) + \tilde{\chi}\mathbf{g}\cdot\hat{\mathbf{n}} + \frac{2}{\tilde{\chi}}\int_0^{\tilde{\chi}}(\Xi + \chi\mathbf{g}\cdot\hat{\mathbf{n}})\,d\chi = 0, \tag{C8}$$

as expected.

3. Perturbation to the expansion history

A less trivial type of perturbation is one in which we alter the cosmic expansion rate. This can be done by setting

$$D = D(\tau) \quad \text{and} \quad E = 0. \tag{C9}$$

The Universe so described is still an FRW model since it is homogeneous and isotropic. (It may no longer be a solution to the Friedmann equation with only matter+Λ, however this does not concern us since we are testing an equation derived only using kinematics.) However, it has a "true" scale factor $a_{\rm true}$ that is related to the unperturbed scale factor via

$$a_{\rm true}(\tau) = a(\tau)[1 + D(\tau) - D(\tau_0)], \tag{C10}$$

where we fix $a_{\rm true}$ to be unity today. The true time coordinate (proper time in the case of FRW) remains equal to the coordinate time,

$$t_{\rm true} = t = \int a(\tau)\,d\tau. \tag{C11}$$

The true conformal time is then

$$\tau_{\rm true} = \int \frac{dt_{\rm true}}{a_{\rm true}} = \int \frac{a\,d\tau}{a_{\rm true}} = \int [1 - D(\tau) + D(\tau_0)]\,d\tau. \tag{C12}$$

(The integration constant is chosen to set $\tau_{\rm true} = 0$ at the Big Bang, but we do not need to make use of this fact.) Integrating gives

$$\tau_{{\rm true},0} - \tau_{\rm true} = [1 + D(\tau_0)](\tau_0 - \tau) - \int_\tau^{\tau_0} D(\tau_1)\,d\tau_1. \tag{C13}$$

We care in particular about the behavior as a function of the observed redshift z, which is related to $a_{\rm true} = (1+\tilde{z})^{-1}$. It follows from Eq. (C10) that the comoving distance relation is now

$$a(\tau) = a_{\rm true}(\tau)[1 - D(\tau) + D(\tau_0)] \tag{C14}$$

and so we may write the perturbation to the conformal time,

$$\tau(a_{\rm true}) = \tau_{\rm bg}(a_{\rm true}) + \frac{D(\tau_0) - D(\tau)}{a_{\rm true}H(a_{\rm true})}. \tag{C15}$$

Here $\tau_{\rm bg}$ is the background conformal time-scale factor relation. Finally using Eq. (C13) yields

$$\tau_{\rm true,0}-\tau_{\rm true} = [1+D(\tau_0)][\tau_{\rm bg}(1)-\tau_{\rm bg}(a_{\rm true})] -\frac{D(\tau_0)-D(\tau)}{a_{\rm true}H(a_{\rm true})}-\int_\tau^{\tau_0}D(\tau_1)\,d\tau_1. \quad (C16)$$

This is the true comoving radial distance $\chi_{\rm true}$ to redshift $a_{\rm true}^{-1}-1$. That is,

$$\chi_{\rm true} = [1+D(\tau_0)]\chi_{\rm bg}(a_{\rm true}) -\frac{D(\tau_0)-D(\tau)}{a_{\rm true}H(a_{\rm true})}-\int_\tau^{\tau_0}D(\tau_1)\,d\tau_1. \quad (C17)$$

The true Hubble rate at this time is

$$\begin{aligned} H_{\rm true} &= \frac{d\ln a_{\rm true}}{dt} \\ &= H(\tau)+\frac{D'(\tau)}{a} \\ &= H_{\rm bg}(a_{\rm true})+\frac{dH}{d\tau}[\tau(a_{\rm true})-\tau_{\rm bg}(a_{\rm true})]+\frac{D'(\tau)}{a} \\ &= H_{\rm bg}(a_{\rm true})+\frac{dH}{d\tau}\frac{D(\tau_0)-D(\tau)}{a_{\rm true}H(a_{\rm true})}+\frac{D'(\tau)}{a} \\ &= H_{\rm bg}(a_{\rm true})+a\frac{dH}{da}[D(\tau_0)-D(\tau)]+\frac{D'(\tau)}{a}. \end{aligned} \quad (C18)$$

We expect the perturbation in the observed galaxy density to have several parts: there is a perturbation in the physical galaxy density, a part associated with the different epoch in cosmic history at which the galaxy density is measured (different t; one wants the different physical density here so we include both the b_e evolution and the -3 associated with the dilution of comoving volume), and a part associated with the different physical volume. Specifically:

$$\tilde\delta_g=\delta_g+(b_e-3)[D(\tau_0)-D(\tau)]+\ln\frac{dV_{\rm true}/da_{\rm true}\,d\Omega}{dV/da\,d\Omega}. \quad (C19)$$

The comoving volume effect is computable from Eq. (C17). We see that

$$\begin{aligned} \frac{dV_{\rm true}}{da_{\rm true}\,d\Omega} &= \frac{a_{\rm true}^2\chi_{\rm true}^2}{H_{\rm true}} \\ &= \frac{a_{\rm true}^2[\chi_{\rm bg}(a_{\rm true})]^2}{H_{\rm bg}(a_{\rm true})}\Big\{1+2D(\tau_0) \\ &\quad -\frac{2\int_\tau^{\tau_0}D(\tau_1)d\tau_1}{\chi(a_{\rm true})}-\frac{2[D(\tau_0)-D(\tau)]}{a_{\rm true}H(a_{\rm true})\chi(a_{\rm true})}\Big\} \\ &\quad \times\Big\{1-\frac{a}{H}\frac{dH}{da}[D(\tau_0)-D(\tau)]-\frac{D'(\tau)}{aH}\Big\}. \end{aligned} \quad (C20)$$

This leads to

$$\begin{aligned} \tilde\delta_g &= \delta_g+(b_e-3)[D(\tau_0)-D(\tau)]+2D(\tau_0) \\ &\quad +\left(-\frac{d\ln H}{d\ln a}-\frac{2}{aH\chi}\right)[D(\tau_0)-D(\tau)] \\ &\quad -\frac{2\int_\tau^{\tau_0}D(\tau_1)d\tau_1}{\chi(a_{\rm true})}-\frac{D'(\tau)}{aH}. \end{aligned} \quad (C21)$$

The expected "magnification" $\delta\mathcal{M}$ is twice the perturbation to the angular diameter distance at fixed observed redshift; in a flat universe this is equivalent to the perturbation to $\chi_{\rm true}$. Using Eq. (C17),

$$\begin{aligned} \delta\mathcal{M} &= -2\frac{\chi_{\rm true}-\chi_{\rm bg}}{\chi_{\rm bg}} \\ &= -2D(\tau_0)+\frac{2[D(\tau_0)-D(\tau)]}{aH\chi_{\rm bg}} \\ &\quad +\frac{2}{\chi_{\rm bg}}\int_\tau^{\tau_0}D(\tau_1)d\tau_1. \end{aligned} \quad (C22)$$

In comparison, if we use Eq. (56) to find $\tilde\delta_g$, then we find that the perturbation in Eq. (C9) yields $\phi=D(\tau)$, $\kappa=0$, and $\delta z=D(\tau_0)-D(\tau)$. Therefore,

$$\begin{aligned} \tilde\delta_g &= \delta_g+\left(b_e-1-\frac{d\ln H}{d\ln a}-\frac{2}{aH\chi}\right)[D(\tau_0)-D(\tau)] \\ &\quad +2D(\tau)-\frac{2\int_\tau^{\tau_0}D(\tau_1)d\tau_1}{\chi}-\frac{D'(\tau)}{aH}. \end{aligned} \quad (C23)$$

A simple comparison shows this to be equivalent to Eq. (C21). Similarly, evaluation of Eq. (73) gives

$$\begin{aligned} \delta\mathcal{M} &= -2D(\tau)+\frac{2}{\tilde\chi}\int_\tau^{\tau_0}D(\tau_1)d\tau_1 \\ &\quad +\left(-2+\frac{2}{aH\chi}\right)[D(\tau_0)-D(\tau)], \end{aligned} \quad (C24)$$

in agreement with Eq. (C22).

4. Spatial curvature

A fourth example of a perturbation we consider is spatial curvature. Under stereographic projection, a 3-sphere of curvature K (radius of curvature $K^{-1/2}$) can be written with 3-metric

$$ds_3^2=\left(1+\frac{1}{4}K|\mathbf{x}|^2\right)^{-2}dx^i dx^i, \quad (C25)$$

or to first order in K,

$$D=-\frac{1}{4}K|\mathbf{x}|^2 \ \text{ and } \ E=0. \quad (C26)$$

The expected result is that in the perturbed universe, the radial comoving distance-redshift relation remains

the same. However, there is a change in the volume element associated with the change in the comoving angular diameter distance,

$$\frac{dV_{\rm new}}{dV_{\rm old}} = \frac{\sin_K^2 \tilde\chi}{\tilde\chi^2} = 1 - \frac{1}{3}K\tilde\chi^2 + \mathcal{O}(K^2), \qquad \text{(C27)}$$

where $\sin_K$ is the sinelike function:

$$\sin_K \chi = \begin{cases} \chi & K = 0 \\ K^{-1/2}\sin(K^{1/2}\chi) & K > 0 \\ (-K)^{-1/2}\sinh[(-K)^{1/2}\chi] & K < 0. \end{cases} \qquad \text{(C28)}$$

Thus we expect to obtain

$$\tilde\delta_g = \delta_g - \frac{1}{3}K\tilde\chi^2. \qquad \text{(C29)}$$

The magnification $\delta\mathcal{M}$ is -2 times the fractional perturbation to the angular diameter distance coming from spatial curvature, which is

$$\delta\mathcal{M} = -2\frac{\sin_K\tilde\chi - \tilde\chi}{\tilde\chi} = \frac{1}{3}K\tilde\chi^2. \qquad \text{(C30)}$$

If we instead use Eq. (56), we find that $\phi = -\frac{1}{4}K\chi^2$, $\kappa = 0$ (since D is a pure monopole, $\nabla_\perp^2 D = 0$ even though $\nabla^2 D \neq 0$), and $\delta z = 0$. Then

$$\tilde\delta_g = \delta_g - \frac{1}{2}K\tilde\chi^2 - \frac{2}{\tilde\chi}\int_0^{\tilde\chi}\left(-\frac{1}{4}K\chi^2\right)\,d\chi. \qquad \text{(C31)}$$

Evaluation of the integral trivially recovers Eq. (C29).

We can also compute the magnification from Eq. (73); we get

$$\delta\mathcal{M} = \frac{1}{2}K\tilde\chi^2 + \frac{2}{\tilde\chi}\int_0^{\tilde\chi}\left(-\frac{1}{4}K\chi^2\right)d\chi = \frac{1}{3}K\tilde\chi^2, \quad \text{(C32)}$$

in agreement with Eq. (C30).

5. Bianchi I cosmology

The previous test cases have not tested the terms involving E'. One case that does is the Bianchi I cosmology, in which the three spatial axes (usually taken to be the coordinate axes) have different scale factors but the universe is still homogeneous. We will focus here on the case where the observer looks in the x^3-direction and the metric perturbations are

$$\begin{aligned} D(\mathbf{x},\tau) &= -s_3(\tau) \ \text{ and} \\ E(\mathbf{x},\tau) &= \frac{s_1(\tau)(x^1)^2 + s_2(\tau)(x^2)^2 + s_3(\tau)(x^3)^2}{2}, \end{aligned} \qquad \text{(C33)}$$

with $s_1(\tau) + s_2(\tau) + s_3(\tau) = 0$ and $s_i(\tau_0) = 0$. This is equivalent to a case where the expansion along the 3-axis is unperturbed, but the other two axes are perturbed: the scale factors are

$$\begin{aligned} a_1(t) &= a(t)[1 + s_1(t) - s_3(t)], \\ a_2(t) &= a(t)[1 + s_2(t) - s_3(t)], \ \text{ and} \\ a_3(t) &= a(t). \end{aligned} \qquad \text{(C34)}$$

Note that we have already considered in Eq. (C9) the case where the global isotropic expansion $D(\tau)$ is perturbed, so no new independent tests of our results are possible by using a different function for D in Eq. (C33). Also we have considered in Eq. (C1) the case where E is a time-independent function with zero Laplacian, so there is no independent test of our result that can be obtained by allowing $s_i(t_0) \neq 0$.

It is straightforward to determine the expected change in observed galaxy density for this model. The metric components $\{g_{00}, g_{03}, g_{33}\}$ are not perturbed, so for the $\hat{\mathbf{n}} = (0,0,1)$ direction the past light cone is unperturbed and a given redshift z corresponds to the usual distance $\chi_{\rm bg}(z)$ and $\tau_{\rm bg}(z)$. The only nontrivial effect is in the transverse dimensions and in the volume element – the angular diameter distance is modified by the perturbed expansion rates in the 1 and 2 directions. We may determine the true angular diameter distance along the 1 axis by considering a ray projected backward from the observer with a physical angular separation ς from the 3-axis, i.e. in direction $\hat{\mathbf{n}} = (\varsigma, 0, 1)$. (We work to order ς so that $\sin\varsigma = \varsigma$ and $\cos\varsigma = 1$.) Then the 4-momentum of such a ray with unit energy is

$$p_\mu = (-1, -\varsigma, 0, -1)\,. \qquad \text{(C35)}$$

Since the metric coefficients do not depend on spatial position in this model, the spatial covariant components p_i of the momentum are conserved. Then we find that the spatial position is given by

$$\begin{aligned} x^1 &= \int_{\tau_0}^{\tau}\frac{dx^1/d\lambda}{dx^0/d\lambda}d\tau_1 \\ &= \int_{\tau_0}^{\tau}\frac{[a_1(\tau_1)]^{-2}p_1}{-[a(\tau_1)]^{-2}p_0}d\tau_1 \\ &= -\varsigma\int_{\tau_0}^{\tau}[1 - 2s_1(\tau_1) + 2s_3(\tau_1)]d\tau_1. \end{aligned} \qquad \text{(C36)}$$

The physical angular diameter distance is the physical transverse distance divided by the angle subtended, i.e. $a_1(\tau)x^1/\varsigma$. That is,

$$\begin{aligned} D_{\rm A,phys,1} &= -a(\tau)[1 + s_1(\tau) - s_3(\tau)] \\ &\quad\times\int_{\tau_0}^{\tau}[1 - 2s_1(\tau_1) + 2s_3(\tau_1)]d\tau_1 \\ &= a(\tau)\Big\{1 + s_1(\tau) - s_3(\tau) \\ &\quad + 2\frac{\int_\tau^{\tau_0}[s_3(\tau_1) - s_1(\tau_1)]d\tau_1}{\tau_0 - \tau}\Big\}. \end{aligned} \qquad \text{(C37)}$$

The observed galaxy overdensity then deviates from the true galaxy overdensity only by the transverse area element (since the time of observation and the longitudinal distance-redshift relation are unaffected). That is,

$$\tilde{\delta}_g = \delta_g + \ln\frac{D_{\rm A,phys,1}D_{\rm A,phys,2}}{D^2_{\rm A,unpert}}. \qquad \text{(C38)}$$

Using that $\sum_{i=1}^3 s_i(\tau) = 0$, we may simplify this to

$$\tilde{\delta}_g = \delta_g - 3s_3(\tau) + 6\frac{\int_\tau^{\tau_0} s_3(\tau_1)d\tau_1}{\tau_0-\tau}. \qquad \text{(C39)}$$

The magnification should also be given by the change in the transverse area element:

$$\delta\mathcal{M} = 3s_3(\tau) - 6\frac{\int_\tau^{\tau_0} s_3(\tau_1)d\tau_1}{\tau_0-\tau}. \qquad \text{(C40)}$$

We now wish to compare our result to Eq. (56). By construction we have on our chosen sightline $D + E_\parallel = 0$, so $\delta z = 0$; and since $\nabla^2 E = 0$ we have $\phi = -s_3$. The convergence κ is more complicated: D is spatially constant, $\nabla^2 E = 0$, and E is a pure quadrupole ($\ell = 2$) and hence $\nabla^2_\perp$ pulls down a factor of $-\ell(\ell+1)/\chi^2 = -6/\chi^2$, so we find

$$\begin{aligned}\nabla^2_\perp\left(D - \frac{1}{3}\nabla^2 E - E''\right) &= -\frac{6E''}{\chi^2} = -\frac{6(s_3''\chi^2/2)}{\chi^2} \\ &= -3s_3'', \end{aligned} \qquad \text{(C41)}$$

where the second equality is valid only on the 3-axis line of sight. Consequently the convergence is

$$\kappa = \frac{3}{2}\int_0^{\tilde\chi} d\chi\,(\tilde\chi-\chi)\frac{\chi}{\tilde\chi}s_3''(\chi). \qquad \text{(C42)}$$

Finally we have $\partial_\parallel^2 E' = s_3'$, and the observer terms $E'(o)$ and $\partial_\parallel E'(o)$ both vanish. Plugging these results into Eq. (56) gives

$$\begin{aligned}\tilde{\delta}_g &= \delta_g - \frac{1+z}{H}s_3'(\tilde\chi) - 2s_3(\tilde\chi) - \frac{2}{\tilde\chi}\left[\frac{1}{2}\tilde\chi^2 s_3'(\tilde\chi)\right] \\ &\quad -\frac{2}{\tilde\chi}\int_0^{\tilde\chi} d\chi\left[-s_3(\chi) + \frac{1}{2}\chi^2 s_3''(\chi)\right] \\ &\quad -3\int_0^{\tilde\chi} d\chi\,(\tilde\chi-\chi)\frac{\chi}{\tilde\chi}s_3''(\chi) \\ &\quad -\frac{1+z}{H}[-s_3'(\tilde\chi)]. \end{aligned} \qquad \text{(C43)}$$

The terms containing $s_3'(\tilde\chi)/H$ cancel and the two integrals can be combined, yielding

$$\begin{aligned}\tilde{\delta}_g &= \delta_g - 2s_3(\tilde\chi) - \tilde\chi s_3'(\tilde\chi) \\ &\quad + \int_0^{\tilde\chi} d\chi\left[\frac{2}{\tilde\chi}s_3(\chi) + \left(2\frac{\chi^2}{\tilde\chi} - 3\chi\right)s_3''(\chi)\right]. \end{aligned} \qquad \text{(C44)}$$

This does not quite resemble Eq. (C39), but we can cast it in a similar form by applying repeated integration by parts to the second derivative term. For a general function f,

$$\begin{aligned}\int_0^{\tilde\chi} f(\chi)s_3''(\chi)d\chi &= -f(\tilde\chi)s_3'(\tilde\chi) + f(0)s_3'(0) \\ &\quad + f'(\tilde\chi)s_3(\tilde\chi) - f'(0)s_3(0) \\ &\quad + \int_0^{\tilde\chi} f''(\chi)s_3(\chi)d\chi, \end{aligned} \qquad \text{(C45)}$$

where the unusual signs result from the fact that $'$ denotes a derivative with respect to τ instead of χ (the relation is simply a minus sign). Then, recalling that $s_3(\chi = 0) = 0$, Eq. (C44) simplifies to

$$\tilde{\delta}_g = \delta_g - 3s_3(\tilde\chi) + \int_0^{\tilde\chi} d\chi\,\frac{6}{\tilde\chi}s_3(\chi). \qquad \text{(C46)}$$

Inspection shows that this is equivalent to Eq. (C39) via a change of variable, $\tau = \tau_0 - \tilde\chi$.

For the magnification, Eq. (73) predicts

$$\begin{aligned}\delta\mathcal{M} &= 2s_3(\tilde\chi) + \tilde\chi s_3'(\tilde\chi) + 3\int_0^{\tilde\chi}(\tilde\chi-\chi)\frac{\chi}{\tilde\chi}s_3''(\chi)\,d\chi \\ &\quad + \frac{2}{\tilde\chi}\int_0^{\tilde\chi}\left[-s_3(\chi) + \frac{1}{2}\chi^2 s_3''(\chi)\right]d\chi; \end{aligned} \qquad \text{(C47)}$$

repeated integration by parts again reduces this to a form equivalent to Eq. (C40).

6. Potential-only mode

The only terms left in Eq. (56) that we have not tested are the observer terms, $E'(o)$ and $\partial_\parallel E'(o)$. These can be tested using a potential-only mode

$$D(\mathbf{x},\tau) = 0 \quad\text{and}\quad E(\mathbf{x},\tau) = \Upsilon(\tau) + w_i(\tau)\,x^i. \qquad \text{(C48)}$$

This mode has no metric perturbation, $D = E_{ij} = 0$, and so we expect to get $\tilde{\delta}_g = \delta_g$. However it does have nonzero observer terms.

Trivial evaluation shows that for the "perturbation" Eq. (C48), we have $\delta z = \phi = 0$. However the convergence κ is *not* zero despite the vanishing metric perturbations! Instead we have

$$\begin{aligned}\kappa &= -\frac{1}{2}\int_0^{\tilde\chi} d\chi\,(\tilde\chi-\chi)\frac{\chi}{\tilde\chi}\nabla^2_\perp(\Upsilon'' + w_i''\hat{n}^i\chi) \\ &= \int_0^{\tilde\chi} d\chi\left(1 - \frac{\chi}{\tilde\chi}\right)w_i''\hat{n}^i, \end{aligned} \qquad \text{(C49)}$$

where in the second line the action of $\nabla^2_\perp$ is to eliminate the monopole and extract a factor of $-2\chi^{-2}$ from the dipole. Now since w_i is a function only of τ we have $w_i'' = d^2 w_i/d\chi^2$. Double integration by parts then gives

$$\kappa = \hat{n}^i w_i'(\tau_0) - \hat{n}^i\frac{w_i(\tau_0) - w_i(\tau_0-\tilde\chi)}{\tilde\chi}. \qquad \text{(C50)}$$

Similarly we find

$$\begin{aligned}\int_0^{\tilde\chi} d\chi\, E'' &= \int_0^{\tilde\chi} d\chi\,(\Upsilon'' + \hat n^i w_i''\chi)\\ &= \Upsilon'(\tau_0) - \Upsilon'(\tau_0-\tilde\chi) - \tilde\chi\hat n^i w_i'(\tau_0-\tilde\chi)\\ &\quad + \hat n^i w_i(\tau_0) - \hat n^i w_i(\tau_0-\tilde\chi). \end{aligned} \tag{C51}$$

Finally the remaining terms are

$$E' - E'(o) = \Upsilon'(\tau_0-\tilde\chi) + \tilde\chi\hat n^i w_i'(\tau_0-\tilde\chi) - \Upsilon'(\tau_0). \tag{C52}$$

and

$$\partial_\parallel E'(o) = \hat n^i w_i'(\tau_0). \tag{C53}$$

Assembling these pieces of Eq. (56) then leads to a mass cancellation that recovers $\tilde\delta_g = \delta_g$, as expected.

The magnification equation, Eq. (73), has the same nonzero pieces and a similar mass cancellation occurs, leaving the correct result $\delta\mathcal{M} = 0$.

Appendix D: Connection with results in the literature

1. Yoo et al.

In this section, we compare our result, Eq. (54),

$$\begin{aligned}\tilde\delta_g(\tilde{\mathbf{x}}) = \delta_g &- (1+\tilde z)\frac{d\ln(a^3\bar n_g)}{dz}\Big|_{\tilde z}\delta z + 2D - E_\parallel\\ &- \left(1 - \frac{1+\tilde z}{H}\frac{dH}{d\tilde z}\right)\delta z - \frac{1+\tilde z}{H(\tilde z)}(D' + E_\parallel')\Big|_{\tilde\chi}\\ &+ 2\frac{\Delta x_\parallel}{\tilde\chi} - 2\hat\kappa \end{aligned} \tag{D1}$$

to Eq. (36) of Yoo et al. [9], restricted to synchronous-comoving gauge:

$$\begin{aligned}\delta_{\rm obs} = b\,(\delta_m - 3\delta z) &+ 2D + E_{ij}\hat n^i\hat n^j\\ &- (1+\tilde z)\frac{\partial}{\partial\tilde z}\delta z - 2\frac{1+\tilde z}{Hr}\delta z - \delta z\\ &- 5p\delta D_L - 2\hat\kappa + \frac{1+\tilde z}{H}\frac{dH}{dz}\delta z + 2\frac{\delta r}{r}. \end{aligned} \tag{D2}$$

We can convert their result to our notation by noting that $r = \tilde\chi$ and

$$\Delta x_\parallel = \delta r - \frac{1+\tilde z}{H(\tilde z)}\delta z. \tag{D3}$$

Note that the δr defined in Eq. (16) of Yoo et al. [9] has a different sign of $E_\parallel$ compared to ours, as discussed in Sec. II. Further, $\partial\delta z/\partial z = 1/H\partial\delta z/\partial\tilde\chi$, and using Eq. (31), Eq. (D2) becomes

$$\begin{aligned}\delta_{\rm obs} = b\,(\delta_m - 3\delta z) &+ 2D + E_\parallel\\ &- \left(1 - \frac{1+\tilde z}{H}\frac{dH}{dz}\right)\delta z - \frac{1+\tilde z}{H(\tilde z)}(D' + E_\parallel')\Big|_{\tilde\chi}\\ &+ 2\frac{\Delta x_\parallel}{\tilde\chi} - 5p\delta D_L - 2\hat\kappa. \end{aligned} \tag{D4}$$

Comparing the two expressions, we find two differences: first, our result involves the time-dependence of the number density of tracers, $d\ln\bar n_g/dz$, while this quantity does not enter Eq. (D4) since the bias is defined in the uniform-redshift gauge (see Sec. III). The second difference is the sign of the $E_\parallel-$term, which goes back to the difference in sign in δr [our Eq. (39), and Eq. (16) in Yoo et al. [9]]. This was discussed in Sec. II.

2. Challinor & Lewis and Bonvin & Durrer

Now we transform our Eq. (56) into variables in conformal Newtonian gauge in order to make comparison with [11] and [13]. By using Eq. (A4), Eq. (A5), Eq. (A10) for gauge transformation of scalar modes respectively in scalar, vector, tensor perturbations, we first find the transformation law from synchronous commoving gauge to conformal Newtonian gauge as

$$\begin{aligned}\Psi = \psi^{\rm (CL)} = \check\alpha &= -E'' - \mathcal{H}E',\\ \Phi = \phi^{\rm (CL)} = -\check\varphi &= -\phi + \mathcal{H}E',\\ \check v &= E',\\ \check{\delta z} &= \delta z + \mathcal{H}E',\\ \check\delta_m &= \delta_m + 3\mathcal{H}E', \text{ and}\\ \check\delta_g &= \delta_g - b_e\mathcal{H}E', \end{aligned} \tag{D5}$$

where the $\check{}$ symbol denotes the quantities in the conformal Newtonian gauge [Eq. (A9)], and the subscript (CL) denotes the metric perturbation variable defined in [11]. Bonvin and Durrer [13] use the Bardeen potentials Ψ, Φ as defined in the above equations. Note that we use $\mathcal{H} \equiv aH$ in order to facilitate the comparison. Now, we make the gauge transform of terms in Eq. (56) as following:

$$\begin{aligned}\delta_g + b_e\delta z &= \check\delta_g + b_e\check{\delta z}\\ \frac{1+z}{H(z)}\partial_\parallel^2 E' &= \frac{1}{\mathcal{H}}\partial_\parallel^2\check v\\ \left(1 - \frac{1+z}{H}\frac{dH}{dz} + \frac{2}{\tilde\chi}\frac{1+z}{H(z)}\right)\delta z &= \left(\frac{\dot{\mathcal{H}}}{\mathcal{H}^2} + \frac{2}{\tilde\chi\mathcal{H}}\right)(\check{\delta z} - \mathcal{H}\check v)\\ 2\phi &= 2(\check\varphi + \mathcal{H}\check v)\\ \frac{2}{\tilde\chi}E' &= \frac{2}{\tilde\chi}\check v\\ \phi + E'' &= -\left(\check\alpha - \check\varphi\right). \end{aligned} \tag{D6}$$

By using the result from Einstein equation, $\phi' = 0$ [Eq. (A26)], and the definition of $\check\kappa$

$$\check\kappa = -\frac{1}{2}\int_0^{\tilde\chi} d\chi\,(\tilde\chi - \chi)\,\frac{\chi}{\tilde\chi}\nabla_\perp^2\,(\check\alpha - \check\varphi) = \kappa, \tag{D7}$$

which is the same as the convergence in conformal Newtonian gauge (κ defined in App. B 2), Eq. (56) becomes

$$\begin{aligned}\tilde{\delta}_g(\tilde{\mathbf{x}}) =& \check{\delta}_g + b_e\check{\delta z} - \frac{1}{\mathcal{H}}\partial_\parallel^2\hat{v} - \left(\frac{\dot{\mathcal{H}}}{\mathcal{H}^2} + \frac{2}{\tilde{\chi}\mathcal{H}}\right)\left[\check{\delta z} - \mathcal{H}\check{v}\right] \\ &+ 2\left[\check{\varphi} + \mathcal{H}\check{v}\right] - \frac{2}{\tilde{\chi}}\check{v} - \frac{2}{\tilde{\chi}}\int_0^{\tilde{\chi}} d\chi\,(\check{\alpha} - \check{\varphi}) - 2\check{\kappa} \\ =& \check{\delta}_g + b_e\check{\delta z} - \frac{1}{\mathcal{H}}\partial_\parallel^2\hat{v} - \left(\frac{\dot{\mathcal{H}}}{\mathcal{H}^2} + \frac{2}{\tilde{\chi}\mathcal{H}}\right)\check{\delta z} \\ &+ 2\check{\varphi} + 3\mathcal{H}\check{v} + \check{\alpha} - \frac{\dot{\check{\varphi}}}{\mathcal{H}} - \frac{2}{\tilde{\chi}}\int_0^{\tilde{\chi}} d\chi\,(\check{\alpha} - \check{\varphi}) - 2\check{\kappa},\end{aligned} \tag{D8}$$

where in the second equality, we use the identity of

$$\frac{\dot{\mathcal{H}}}{\mathcal{H}}\check{v} = \check{\alpha} + \mathcal{H}\check{v} - \frac{\dot{\check{\varphi}}}{\mathcal{H}}, \tag{D9}$$

and we drop the quantities at observers position as is done by [11].

The redshift perturbation $\check{\delta z}$ in conformal Newtonian gauge can be calculated from from Eq. (B5) and gauge transformation Eq. (D5) as

$$\check{\delta z} = \partial_\parallel\check{v} - \check{\alpha} - \int_0^{\tilde{\chi}} d\chi\,(\check{\alpha} - \check{\varphi})'. \tag{D10}$$

Rewriting the equation in terms of the variables in Challinor and Lewis [11] ($\check{\alpha} = \psi$, $\check{\varphi} = -\phi$, and $\partial_\parallel\check{v} = \mathbf{v}\cdot\hat{\mathbf{n}}$), we find the redshift perturbation as

$$\check{\delta z} = \mathbf{v}\cdot\hat{\mathbf{n}} - \psi^{(\mathrm{CL})} - \int_0^{\tilde{\chi}} d\chi\left(\psi^{(\mathrm{CL})} + \phi^{(\mathrm{CL})}\right)'. \tag{D11}$$

Similar change of variables can be made for the observed galaxy density contrast in Eq. (D8), which yields

$$\tilde{\delta}_g(\tilde{\mathbf{x}}) = \Delta_n(\hat{\mathbf{n}}, z) + 3\mathcal{H}\check{v} \tag{D12}$$

where $\Delta_n(\hat{\mathbf{n}}, z)$ is in Eq. (30) of Challinor and Lewis [11]. The additional term of $3\mathcal{H}\check{v}$ is due to the fact that the overdensities Δ_n and Δ are defined with respect to the physical, rather than comoving galaxy density. In performing the gauge transformation $t \to \check{t} = t + T$, we thus obtain an addition term from $\ln\check{a}^3 = \ln a^3 + 3aHT = \ln a^3 + 3\mathcal{H}\check{v}$.

To compare the magnification terms, we transform Eq. (73) to the conformal Newtonian gauge as

$$\begin{aligned}\delta\mathcal{M} =& -2(\check{\varphi} + \mathcal{H}\check{v}) + \frac{2}{\tilde{\chi}}\check{v} + 2\check{\kappa} - \frac{2}{\tilde{\chi}}\int_0^{\tilde{\chi}} d\chi\,(\check{\alpha} - \check{\varphi}) \\ &- 2\left(1 - \frac{1}{\mathcal{H}\tilde{\chi}}\right)\left(\check{\delta z} - \mathcal{H}\check{v}\right) \\ =& 2\kappa + 2\phi^{(\mathrm{CL})} - \frac{2}{\tilde{\chi}}\int_0^{\tilde{\chi}} d\chi\left(\phi^{(\mathrm{CL})} + \psi^{(\mathrm{CL})}\right) \\ &+ 2\left(\frac{1}{\mathcal{H}\tilde{\chi}} - 1\right)\check{\delta z},\end{aligned} \tag{D13}$$

which has to be compared to all terms $\propto 5s$ in Eq. (37) of [11]:

$$\begin{aligned}&\kappa - \frac{1}{\tilde{\chi}}\int d\chi(\phi + \psi) + \phi \\ &+ \left(\frac{1}{\mathcal{H}\tilde{\chi}} - 1\right)\left[-\psi - \int d\chi(\phi' + \psi') + \hat{n}\cdot v\right]\end{aligned} \tag{D14}$$

As their $5s$ is the same as $2\mathcal{Q}$ in our notation, our formula for $\delta\mathcal{M}$ also agrees with theirs.

We can also write Eq. (D8) in terms of the variables in Bonvin and Durrer [13],

$$\begin{aligned}\check{\delta}_g + b_e\check{\delta z} =& D_s, \\ \check{\alpha} =& \Psi, \\ \check{\varphi} =& -\Phi, \\ \partial_\parallel\check{v} =& -\mathbf{V}\cdot\hat{\mathbf{n}}, \quad \text{and} \\ \partial_\parallel^2\check{v} =& \partial_r\left(\mathbf{V}\cdot\hat{\mathbf{n}}\right),\end{aligned} \tag{D15}$$

to arrive at the same relation Eq. (D12), after identifying

$$\kappa = \frac{1}{2r_S}\int_0^{r_S} dr\left[\frac{r_S - r}{r}\Delta_\Omega\right](\Phi + \Psi) \tag{D16}$$

and $\Delta_n = \Delta$ as defined in Ref. [13].

[1] N. Dalal, O. Doré, D. Huterer, and A. Shirokov, Phys. Rev. D **77**, 123514 (2008), 0710.4560.

[2] A. Slosar, C. Hirata, U. Seljak, S. Ho, and N. Padmanabhan, JCAP **8**, 31 (2008), 0805.3580.

[3] D. J. Eisenstein, D. H. Weinberg, E. Agol, H. Aihara, C. Allende Prieto, S. F. Anderson, J. A. Arns, E. Aubourg, S. Bailey, E. Balbinot, et al., ArXiv e-prints (2011), 1101.1529.

[4] G. J. Hill, K. Gebhardt, E. Komatsu, N. Drory, P. J. MacQueen, J. Adams, G. A. Blanc, R. Koehler, M. Rafal, M. M. Roth, et al., in *Panoramic Views of Galaxy Formation and Evolution*, edited by T. Kodama, T. Yamada, & K. Aoki (2008), vol. 399 of *Astronomical Society of the Pacific Conference Series*, pp. 115–+, 0806.0183.

[5] D. Schlegel, F. Abdalla, T. Abraham, C. Ahn, C. Allende Prieto, J. Annis, E. Aubourg, M. Azzaro, S. B. C. Baltay, C. Baugh, et al., ArXiv e-prints (2011), 1106.1706.

[6] R. K. Sachs and A. M. Wolfe, Astrophys. J. **147**, 73 (1967).

[7] M. Sasaki, Mon. Not. R. Astron. Soc. **228**, 653 (1987).

[8] C. Bonvin, R. Durrer, and M. A. Gasparini, Phys. Rev. D **73**, 023523 (2006), arXiv:astro-ph/0511183.

[9] J. Yoo, A. L. Fitzpatrick, and M. Zaldarriaga, Phys. Rev. D **80**, 083514 (2009), 0907.0707.

[10] J. Yoo, Phys. Rev. D **82**, 083508 (2010), 1009.3021.
[11] A. Challinor and A. Lewis, ArXiv e-prints (2011), 1105.5292.
[12] M. Bruni, R. Crittenden, K. Koyama, R. Maartens, C. Pitrou, and D. Wands, ArXiv e-prints (2011), 1106.3999.
[13] C. Bonvin and R. Durrer, ArXiv e-prints (2011), 1105.5280.
[14] S. Dodelson, F. Schmidt, and A. Vallinotto, Phys. Rev. D **78**, 043508 (2008), 0806.0331.
[15] C. M. Hirata, JCAP **9**, 11 (2009), 0907.0703.
[16] F. Schmidt, E. Rozo, S. Dodelson, L. Hui, and E. Sheldon, Physical Review Letters **103**, 051301 (2009), 0904.4702.
[17] P. McDonald and A. Roy, JCAP **8**, 20 (2009), 0902.0991.
[18] C. M. Hirata, Mon. Not. R. Astron. Soc. **399**, 1074 (2009), 0903.4929.
[19] N. Kaiser, Astrophys. J. Lett. **284**, L9 (1984).
[20] H. J. Mo and S. D. M. White, Mon. Not. R. Astron. Soc. **282**, 347 (1996), arXiv:astro-ph/9512127.
[21] B. A. Reid, L. Verde, K. Dolag, S. Matarrese, and L. Moscardini, JCAP **7**, 13 (2010), 1004.1637.
[22] N. Kaiser, Mon. Not. R. Astron. Soc. **227**, 1 (1987).
[23] N. E. Chisari and M. Zaldarriaga, ArXiv e-prints (2011), 1101.3555.
[24] E. Komatsu, K. M. Smith, J. Dunkley, C. L. Bennett, B. Gold, G. Hinshaw, N. Jarosik, D. Larson, M. R. Nolta, L. Page, et al., Astrophys. J. Supp. **192**, 18 (2011), 1001.4538.
[25] F. Schmidt, Phys. Rev. D **82**, 063001 (2010), 1005.4063.
[26] T. Baldauf, U. Seljak, L. Senatore, and M. Zaldarriaga, ArXiv e-prints (2011), 1106.5507.
[27] V. Desjacques, D. Jeong, and F. Schmidt, ArXiv e-prints (2011), 1105.3628.
[28] F. Schmidt and M. Kamionkowski, Phys. Rev. D **82**, 103002 (2010), 1008.0638.
[29] D. Wands and A. Slosar, Phys. Rev. D **79**, 123507 (2009), 0902.1084.
[30] J. M. Bardeen, Phys. Rev. D **22**, 1882 (1980).
[31] C. Ma and E. Bertschinger, Astrophys. J. **455**, 7 (1995), arXiv:astro-ph/9506072.
[32] W. Hu and A. Cooray, Phys. Rev. D **63**, 023504 (2000).